Cellular Signalling xxx (2016) xxx-xxx

Contents lists available at ScienceDirect

Cellular Signalling

journal homepage: www.elsevier.com

Nitric oxide-coupled signaling in odor elicited molecular events in the olfactory center of the terrestrial snail, *Helix pomatia*☆

Zoltán Serfőző[a, *, 1], Kálmán Nacsa[a, 1], Zoltán Veréb[b], Izabella Battonyai[a], Csaba Hegedűs[c], Csilla Balogh[a], Károly Elekes[a]

[a] *MTA Centre for Ecological Research, Balaton Limnological Institute, Tihany, Hungary*
[b] *Institute of Biochemistry and Molecular Biology, Medical and Health Science Center, University of Debrecen, Debrecen, Hungary*

http://dx.doi.org/10.1016/j.cellsig.2016.11.017
0898-6568/

[c] *Institute of Medical Chemistry, Medical and Health Science Center, University of Debrecen, Debrecen, Hungary*

ARTICLE INFO

Article history:
Received 1 September 2016
Received in revised form 15 November 2016
Accepted 18 November 2016
Available online xxx

Keywords:
AGC family kinase
Cyclic guanosine monophosphate
Glutamate
Nitric oxide
Olfaction
Procerebrum

ABSTRACT

Olfaction, a chemosensory modality, plays a pivotal role in the orientation and behavior of invertebrates. The central olfactory processing unit in terrestrial stylomatophoran snails is the procerebrum, which contains NO synthesizing interneurons, whose oscillatory currents are believed to be the base of odor evoked memory formation. Nevertheless, in this model the up- and downstream events of molecular cascades that trigger and follow NO release, respectively, have not been studied. Immunocytochemistry and flow cytometry studies performed on procerebral neural perikarya isolated from the snail *Helix pomatia* revealed cell populations with discrete DAF-2 fluorescence, indicating the release of different amounts of NO. Glutamate increased the intensity of DAF-2 fluorescence, and the number of DAF-2 positive non-bursting interneurons, through a mechanism likely to involve an NMDA-like receptor. Similarly to glutamate, NO activation induced an increase in intracellular cGMP levels through activation of soluble guanylyl cyclase. Immunohistochemical localization of proteins possessing the phosphorylated target sequence of AGC family kinases (RXXS/T-P), among them protein kinase A (RRXS/T-P), showed striking similarities to the distribution of NOS/cGMP. Activators of cyclic nucleotide synthesis increased the AGC-kinase-dependent phosphorylation of discrete proteins with 28, 45, and 55 kDa mw. Importantly, exposure of snails to an attractive odorant induced hyperphosphorylation of the 28 kDa protein, and increased levels of cGMP synthesis. Protein S-nitrosylation and intercellular activation of protein kinase G were also suggested as

1. Introduction

The sense of olfaction is particularly important in invertebrates in which other sensory modalities, such as vision and hearing, are less developed. For example, odor-based sensation in gastropod mollusks plays a critical role in guiding behaviors such as food location, predator/danger avoidance, and sexual attraction [1,2]. Terrestrial stylommatophoran snails have a specialized olfactory organ called the ommatophores (or the upper or posterior tentacles), located at the upper end of the tentacles, which scan scents in the air when the animal is active [1]. Olfactory stimuli detected by the ommatophores are then relayed to the olfactory center in the CNS, called the procerebrum (PC) [1]. The cellular organization and physiology of the mammalian olfactory bulb and the snail PC share many similarities, including the mechanism of odor processing, acquisition, memory formation and the related foraging behavior. In terrestrial snails great attention has been paid to olfaction and olfactory behavior, hence they became one of the major objects of many studies in the past decades [1]. In particular, the PC has become recognized as an ideal model system for comparative studies dealing with the neurobiological background of odor processing. Knowledge of central processing mechanism for odor information in stylommatophoran snails, and in particular the slug *Limax* sp., has recently been reviewed extensively [3].

According to results obtained on slugs (*Limax* sp., *Lehmannia* sp. [3]), and snails (*Helix* spp. [4], *Achatina fulica* [5]), the cellular organization of PCs from different molluscs share a number of common features. Track tracing experiments have revealed the members of the neuronal afferents and the types and morphology of PC interneurons [5,6,7,8,9,10]. In addition to morphological findings, electrophysiological recording has also demonstrated that the population of PC cells within the layer where the perikarya of PC interneurons are located (the cell mass layer) consists of large number (75%) of non-bursting (NB) neurons with small size (5–8 μm), and a smaller number (25%) of bursting (B) neurons of larger size (10–15 μm) [11,12].

Projections of NB cells receive input via the tentacular nerve in the terminal neuropil (TN), and transmit this information in a frequency code of propagated oscillatory waves to PC neuropil areas (TN and internal neuropil [IN, [13,14]). Spontaneous oscillation of the local field potentials (LFPs) in PCs propagate from the apical to the basal end, with frequency of the LFPs exhibiting a sensitivity to bursting activity stemming from B cells. B cells send multipolar projections oriented perpendicular to the direction of wave propagation, and interconnecting many NB cell perikarya within the cell mass layer [15]. Changes in the LFP oscillation pattern and frequency have been proposed to encode the type and intensity of odor stimulus, in a manner sensitive to the current functional state of the PC neuronal net-

Abbreviations: 5-HT, 5-hydroxytryptamine or serotonin; ACh, acetylcholine; AGC-S-P, phosphorylated substrate of the AGC-family protein kinase; Akt, protein kinase B; AMPA, α-amino-3-hydroxy-5-methyl-4-isoxazolepropionic acid; APV, (2*R*)-amino-5-phosphonovaleric acid; B cell, large bursting neuron in the procerebrum; β-NADP, β-nicotinamide adenine dinucleotide; β-NADPH, β-nicotinamide adenine dinucleotide 2′-phosphate; BSA, bovine serum albumin; cAMP, 3′,5′-cyclic adenosine monophosphate; cGMP, 3′,5′-cyclic guanosine monophosphate; CNG channel, cyclic nucleotide-gated ion channel; CNQX, 6-cyano-7-nitroquinoxaline-2,3-dione; CNS, central nervous system; DAB, 3,3′-diaminobenzidine; DAF-2-DA, 4,5-diaminofluorescein diacetate; DAF-2, 4,5-diaminofluorescein; DMSO, dimethyl sulfoxide; EDTA, ethylenediaminetetraacetic acid; ELISA, enzyme-linked immunosorbent assay; FACS, fluorescence-activated cell sorting; GABA, γ-aminobutyric acid; Glu, glutamate; GluR, glutamate receptor; GSNO, S-nitrosoglutathione (2-amino-5-{[1-(carboxymethylamino)-3-nitrososulfanyl-1-oxopropan-2-yl]amino}-5-oxopentanoic acid); HCN channel, hyperpolarization-activated cyclic nucleotide-gated ion channels; HEPES buffer, 4-(2-hydroxyethyl)-1-piperazineethanesulfonic acid; HPS, *Helix pomatia* physiological solution; HRP, horseradish peroxidase; IBMX, 3-isobutyl-1-methylxanthine; ICC, immunocytochemistry; IHC, immunohistochemistry; IN, internal neuropil; IR, immunoreactive; IPSP, inhibitory postsynaptic potential; KOH, potassium hydroxide; LFP, local field potential; L-NAME, Nω-Nitro-L-arginine methyl ester; MK-801, (5*S*,10*R*)-(+)-5-Methyl-10,11-dihydro-5H-dibenzo[*a*,*d*]cyclohepten-5,10-imine hydrogen maleate; mw, molecular weight; NB cell, small non-bursting neuron in the procerebrum; NBQX, 2,3-dihydroxy-6-nitro-7-sulfamoyl-benzo[*f*]quinoxaline-2,3-dione or 2,3-dioxo-6-nitro-1,2,3,4-tetrahydrobenzo[*f*]quinoxaline-7-sulfonamide; NMDA, *N*-methyl-D-aspartic acid; NO, nitric oxide; NO_2^-, nitrite; NO_3^-, nitrate; NO_x, nitrogen oxides; NOS, nitric oxide synthase; PAGE, polyacrylamide gel electrophoresis; PAPANONOate, 3-(2-hydroxy-2-nitroso-1-propylhydrazino)-1-propanamine; PBS, phosphate-buffered saline; PC, procerebral lobe, procerebrum; PFA, paraformaldehyde; PKA, protein kinase A; PKA-S-P, phosphorylated substrate of the protein kinase A; PKC, protein kinase C; PKG, protein kinase G; RIPA buffer, radio-immunoprecipitation assay buffer; SDS, sodium dodecyl sulfate; sGC, soluble guanylyl cyclase; SNAP, S-nitroso-*N*-acetylpenicillamine; SNP, sodium nitroprusside; TBS, Tris-HCl buffered saline; TCA, trichloroacetic acid; TN, terminal neuropil; Tris-HCl, tris(hydroxymethyl)aminomethane hydrochloride; TritonX-100, 4-(1,1,3,3-tetramethylbutyl)phenyl-polyethylene glycol; Tween-20, polyoxyethylene (20) sorbitan monolaurate; vGluT, vesicular glutamate transporter; YC-1, 3-(5′-hydroxymethyl-2′-furyl)-1-benzyl indazole

[?] Author's contribution to the paper: This study was designed, directed and coordinated by Z.S., as the principal investigator. Z.S. provided conceptual and technical guidance for all aspects of the project. Z.S. planned and carried out the experiments, financed the study, and wrote the manuscript. K.N. performed immunohisto- and cytochemical, Western blot and behavioral experiments, and was co-first author of the manuscript. Z.V. carried out flow cytometry experiments and analyzed the data. I.B. contributed to immunohistochemistry. C.H. performed the nitric oxide measurements. C.B. carried out statistical analysis. K.E. financed the research and corrected the manuscript. The manuscript was agreed to by all authors.

* Corresponding author at: Klebelsberg Kuno u. 3, Tihany, H-8237, Hungary.
Email address: serfozo.zoltan@okologia.mta.hu (Z. Serfőző)

[1] Z.S. and K.N. equally contributed to the work.

alternative components of NO signaling in the snail procerebrum. The present results from *Helix pomatia* indicate an important role for procerebrum NO/cGMP/PKA signaling pathways in the regulation of olfactory (food-finding) behavior.

work [16]. NB cells in the PC form direct connections with the afferents of neurons in the buccal and pedal ganglia feeding circuitry [17], providing evidence for a significant role of olfaction in behavioral (feeding) responses [18].

Reciprocal chemical communication between NB and B cells, and possible electric coupling between B cells, were suggested [19]. Synaptic contacts were rarely found in the PC [20,21,22], instead axo-somatic and axo-axonic forms of unspecialized but close membrane contacts, typical of the snail CNS, frequently occurred [22]. Various types of transmitter-containing vesicles and granules in the axon profiles [22] were also described. The presence of neurotransmitters (glutamate, Glu [and its vesicular transporter, vGluT, 23], GABA [24,25], 5-HT [22], nitric oxide [NO, 26, 27, 28], acetylcholine [29], histamine [30]), and different neuropeptides [31,32,33,34,35] were demonstrated immunohistochemically. This, together with the findings on their effect following exogenous application [23,29,30,35,36,37,38,39,40], underlined the complex intrinsic and extrinsic regulation of neuronal activity in the PC.

Among the intrinsic neurotransmitters Glu and NO seem to be the key signal molecules regulating LFP oscillation. In *Limax* sp., Glu and NOS were demonstrated in both B and NB cells, even if the main source of Glu was proposed to be B cells, and the majority of mRNAs of NO synthase (NOS) isoforms (*lim*$NOS_{1,2}$) were found in NB cells [23,41,42,43]. Exogenous applications of Glu or NO provoked a synergistic network oscillation [23,26], and Glu and NO, respectively, evoked a train of IPSPs in NB cells, and simultaneously increased the bursting frequency of B cells [23,26]. As a result, it is hypothesized that both transmitters evoke an enhanced frequency of LFP oscillation through exciting the inhibitory activity of B cells on NB cells. The actions of Glu on B cells involved Glu receptor (GluR)-coupled excitatory Cl^- fluxes [44], while Glu stimulated inhibitory K^+ channels on NB cells [11,13]. On the other hand, it is still not clear which type(s) of known GluR participate in transmitting Glu signals to PC neurons. The specific AMPA-receptor blocker NBQX had no effect on LFP oscillation, and the GluR2 subunit, which is a constitutive part in most of this type of GluR in the mammalian CNS, is not expressed in the PC [23]. However, no evidences have yet been provided for the presence of other, NMDA or kainate receptor types. Similarly to Glu release, Ca^{2+} transients also showed rhythmic activity in the PC [45], implying the possibility of integration of an NMDA-type Ca^{2+} ionophore in the membrane of PC neurons. NMDA-like receptors were sequenced and cloned from two non-stylommatophoran, heterobranch mollusks: the sea hare, *Aplysia californica* (*Ac*GluR1, accession number: AAO62106) and the pond snail, *Lymnaea stagnalis* (*Ls*GluR1, accession number: AY571900, [46]). Predicted transcripts of these putative NMDA-receptor sequences showed similarities (glycine and Glu binding sites, postsynaptic density protein [PDZ]-domain) to the mammalian GluN1 subunit. However, pharmacological experiments showed that *Lymnaea stagnalis* NMDA-like receptor was insensitive to the mammalian NMDA channel antagonist APV, and did not exhibit the voltage-dependent Mg^{2+}-blockage typical of NMDA-type channels [47]. It is not known whether the coupling between Glu and NO occurs in the PC. However, in *Lymnaea stagnalis* NO level has been shown to switch the inhibitory action of Glu into excitation in the feeding network of the buccal ganglion [48] through a mechanism involving NMDA-like receptors [49].

NO signaling in the nervous system is generally accepted to involve the binding of NO to its receptor, soluble guanylyl cyclase (sGC), followed by the generation of the second messenger, cyclic guanosine monophosphate (cGMP), which then activates the cGMP-dependent protein kinase (PKG), phosphodiesterases, and cyclic nucleotide-gated (CNG) ion channels [50]. PKG widens the nitrergic pathway by the potential phosphorylation of a number of proteins, including a small number that can also be involved in PKG activation [51]. Alternatively, NO can directly nitrosylate specific protein cystein residues, forming S-nitrosothiols, which have a modulatory role at glutamatergic synapses, affecting synaptic vesicle release and NMDA-receptor inactivation [52]. Although NOS gene evolution and NO neurotransmitter actions have been studied intensively [53,54], the different elements of NO signaling have received little attention in invertebrates [54]. In mollusks, the canonical NO/cGMP/PKG pathway was detected in the regulation of growth cone filopodial dynamics of cultured neuron of *Helisoma trivolvis* [55]. In addition to NO, the presence of sGC and PKG was also confirmed in *Aplysia* sp., along with a potential role for these enzymes in the molecular machinery of the gill-withdrawal reflex [54]. *Limax* sp. and *Lymnaea stagnalis* sGC isoforms and subunits were cloned and shown to be associated with NO signaling in the olfactory system, and in an identified modulatory neuron regulating the feeding program [42,56,57]. In the appetitive behavior of *Lymnaea stagnalis* the NO-cGMP step was required in the course of early events of memory acquisition [58]. However, both in *Aplysia* sp. and *Lymnaea stagnalis* PKG seemed to be separated in time and space from the activation of NO/cGMP [54,59]. Similarly to that found in the honeybee, *Apis mellifera* [60], PKA rather than PKG is involved in this cascade in *Lymnaea stagnalis* where it plays a pivotal role in associative learning [59]. PKA, PKG and PKC are the core members of the AGC family Ser/Thr kinases, which share substrate specificity, and the minimum requirement of an arginine (R) at the − 3′ position relative to the phosphorylated Ser/Thr (RXXS/T). A number of proteins, contributing to various functions, can be found in mammals that contain the target sequence for AGC family kinases, and which are highly conserved in other homologue proteins of lower Metazoan groups [61]. Recently, a hyperpolarization-activated, CNG cation channel (HCN), has been cloned and characterized in *Aplysia* sp. inter- and motoneurons [62], which mediated an inward K^+ current following NO-stimulated cGMP synthesis. Work in the CNS of *Sepia officinalis* has also identified an alternative, direct regulatory effect, of NO, involving tyrosine nitration [63].

Overall, it is not fully clear what molecular mechanisms precede and follow NO liberation in these invertebrate model systems. Therefore, in the present study, we investigated the inducers and downstream chemical cascades of nitrergic signaling in the well established model of central olfactory processing, the PC of *Helix pomatia*. NOS was localized in the *Helix* spp. PC [27,28,64,65], with applications of NO inducing reliable increases in cGMP synthesis [66]. Moreover, NOS inhibition was found to impair food-finding behavior, suggesting a role for NO signaling in *Helix pomatia* olfaction [67]. We used flow cytometry analysis of the NO acceptor fluorescent dye, DAF-2-DA, which is suitable for NO detection in mollusks [68], to characterize NO activity in PC neurons. A battery of selected antibodies, raised against the putative participants of the NO cascade, were applied in different immunological techniques, such as immunohistochemistry, Western blot and ELISA, to identify and characterize NO-coupled processes within the PC. Finally, we compared protein phosphorylation occurring following NO application ex vivo, and odorant stimulation in vivo.

2. Materials and methods

2.1. NO measurement

The tissue level of NO was determined from its oxidized metabolites (NO_x: NO_2^-, NO_3^-). Twenty four PCs obtained from 12 specimens of the snail, *Helix pomatia*, were extracted in a mixture of 80 μl cell lysating radio-immunoprecipitation assay (RIPA) buffer (1% [v/v] Nonidet P-40, 1% [w/v] sodium deoxycholate, 0.15 M NaCl, 0.01 M sodium phosphate [pH 7.2], 2 mM EDTA, 50 mM sodium fluoride, and protease inhibitor [Sigma-Aldrich, cat. # P8340, Budapest, Hungary]), from which 4 μl sample (protein content: 1,7 mg) was taken out and used for NO_x species production propagated by activating NOS with a NADPH regenerating system (constituent of the Ultrasensitive Colorimetric NOS Assay Kit, Oxford Biomedical Research, cat. # NB78, Oxford, MI). Following the manufacturer's protocol, 4 μl sample was incubated in 4 μl 50 mM HEPES buffer (pH 7.5) containing 0.5 mM EDTA, and NADP, glucose-6-phosphate, glucose-6-phosphate dehydrogenase in a concentration adjusted by the company, for 3 h at room temperature. The reaction was stopped with inactivation of the enzyme activity by adding 8 μl 96% ethanol at 0 °C for 30 min. Denatured proteins were removed by centrifugation for 5 min at 10,000*g*. 100 μl samples were injected into a sealed glass set-up of the Sievers NO Analyzer instrument (NOA, 280i, GE, Boulder, CO), in which NO_2^- was reduced to NO by 1% [w/v] NaI in glacial acetic acid. NO was detected based on a gas phase chemiluminescence reaction of NO with ozone (for details see http://www.geinstruments.com/library/manuals/nitric-oxide-analyzer--noa--documentation.html, accessed: 25.10.2012, p. 15). Signals were quantified using a freshly prepared and tested NO_2^- standard. Data were obtained from three different measurements.

2.2. Microscopic visualization of NO

NO production of PC cells was visualized by the fluorescent NO-acceptor dye 4,5-diaminofluorescein diacetate dissolved in DMSO (5 mM DAF-2-DA solution, cat. # D225 Sigma-Aldrich). To obtain separated PC neurons, isolated PCs were dissociated with the use of a 200 μl pipette tip and a pipettor by gentle forcing in 100 μl *Helix pomatia* physiological saline (HPS, 111.1 mM NaCl, 1.87 mM KCl, 1.08 mM $CaCl_2$, 2.38 mM Na_2CO_3, pH 7.4). Both cell suspension and desheathed PCs were incubated with 10 μM DAF-2-DA diluted in HPS in darkness at room temperature for 15 min, then examined and counted under a fluorescence microscope at 490/525 nm excitation/emission filter combinations as cell smears or whole-mount preparations. In those parts of the slide where they homogeneously distributed all intact cells up to 300 counts were registered by following a meander line. Three pairs of PC were examined, respectively. Specificity of the NO-DAF-2 reaction was tested by measuring the fluorescence of HPS without or with cells in the presence or absence of DAF-2-DA in three parallel experiments. For specificity, control cells were pulse sonicated in darkness with an ultrasonic homogenizer (Cole Palmer, cat. # 8852, London, U.K.) and centrifuged at 2000*g*, at 4 °C. DAF-2 fluorescence intensity was measured from the supernatant and HPS with 485/600 nm excitation/emission wavelength filters, in a Victor^3 Multi Label Counter (PerkinElmer, Waltham MA).

2.3. Flow cytometry

PC cells were isolated from 2 to 3 PCs as described in Section 2.2. DAF-2-DA containing solution was added to the suspension in a final concentration of 0.5 μM and the suspension was incubated for 10 min at room temperature. When the NO production was investigated in the presence of different chemical substances the cells were incubated with the chemical or chemical combinations for 15 min prior to DAF-2-DA exposition. The following chemicals (all from Sigma-Aldrich) were used: 1 μM β-NADPH (cat. # N9910), 5 μl arginine substrate solution (cat. # A4344), 100 μM L-NAME (cat. # N5751), 10 μM L-Glu (cat. # G1626), 10 μM MK-801 (cat. # M107), 10 μM ACh (cat. # A6625). Chemical concentrations used were optimized first in preliminary experiments in order to apply those minimum values which provoke definitive effect and also, have physiological relevance. The suspension was mixed with 300 μl Fluorescence-Activated Cell Sorting (FACS) buffer, and DAF-2 fluorescent intensity of cells was measured by FACSCalibur flow cytometer (BD Biosciences, Franklin Lakes, NJ). Baseline was recorded in dye free and also in dye containing cell suspension (controls). Each experiment was repeated five times with at least 20×10^5 counted cells, obtained in each case from 10 to 15 animals. The data were analyzed using Flowing Software (Cell Imaging Core, Turku Centre for Biotechnology, Turku Finland).

2.4. Western blotting

Six PCs obtained from three snails were homogenized in a standard, 0.1% (w/v) SDS-containing lysating (RIPA) buffer, to which 1% (v/v) protease inhibitor cocktail [Sigma-Aldrich, cat. # P8340; P0044] was added, and then centrifuged at 10,000 *g* for 5 min. Aliquots of the supernatant were immediately used or kept frozen at − 80 °C until use. When the effect of NO on protein S-nitrosylation or protein-phosphorylation by AGC family kinases was studied ex vivo prior to homogenization, the isolated PCs were incubated with chemical substances dissolved in HPS in darkness at room temperature for 10 min. The following chemicals were used in 100 μM concentration: SNP, SNAP, IBMX, forskolin, GSNO (all from Sigma-Aldrich). Forskolin was dissolved first in DMSO (1.4% [w/v]). Protein concentration was determined by the BCA assay (Pierce, cat. # 23225, ThermoFisher Sci., Waltham, MA). Proteins (50 μg/each sample) were resolved in the standard 1 × SDS-containing loading buffer (2% [w/v] SDS, 0.2% [w/v] bromophenol blue, 20% [v/v] glycerol, 200 mM dithiothreitol in 100 mM Tris-HCl, pH 6.8), and separated with polyacrylamide gel electrophoresis (PAGE). Proteins were blotted onto nitrocellulose membranes which were subsequently blocked by 5% non-fat milk or BSA in 1 × TBS-Tween (50 M Tris-HCl buffered saline, pH 7.6, 0.1% Tween-20), depending on the protocol of the primary antibody producer. Details of the primary antibodies are given in Table 1. Whole membranes or cut strips were incubated with the primary antibodies overnight at 4 °C, and then labeled with HRP-conjugated secondary antibodies, corresponding to the primary antibody, for 1 h at room temperature. Details of the primary and secondary antibody pairs can be found in Table 2. Visualization of the immunocomplex was carried out with a Pierce enhanced chemiluminescent Western blotting substrate for HRP (Pierce, 32106, ThermoFisher Sci., Waltham, MA). Substitution of the primary antibody with normal rabbit, mouse, or goat serum (Dako, cat. # X0902, X0910, X0907, Agilent Tech. Santa Clara, CA) was used as control. CNS extract of *Lymnaea stagnalis* was used as a positive control testing the anti-NMDA receptor antibody, since the *Lymnaea stagnalis* NMDA receptor was sequenced [46].

During the evaluation of Western blot results we considered the immunoreaction to be specific for the target or "target-like protein" if the labeled band (i) was repetitively detected in subsequent experiments; (ii) could be distinguished from secondary bands; (iii) the mol-

Table 1

Antibody name and ID	Producer	Product number	Epitope	Type, source	Homology with known mollusk sequences	Applied concentration in WB (and in IHC)
NMDAζ1 AB_2112157	Santa Cruz, Biotech. Inc., CA	sc-31556	R-20 internal region of human NMDAζ1	Polyclonal goat IgG	79% homology with the sequence alignment of the cloned *Lymnaea stagnalis* NMDA receptor internal region (ACC95432.1, [46]). According to correspondence with the producer	1:200 (1:50)
GCS-β-1 AB_675606	Santa Cruz, Biotech. Inc., CA	sc-34430	G-14 near the C-terminus of human GCS-β-1	Polyclonal goat IgG	100% homology with the sequence alignment of the cloned *Lymnaea stagnalis Lym*-sGCb1 C-terminus (EU624340, [56]). According to correspondence with the producer	1:200 (1:50)
PKG-1 AB_2067450	Cell Signaling Technology, Danvers, MA	ab3248	Peptide from the conservative central residues of the human PKG-1, with wide species cross-reactivity	Rabmab IgG	high (87%) coincidence with the corresponding predicted protein sequence of the *Aplysia californica* transcribed mRNA of the PKG-1 like protein (GBBE01011458.1)	1:1000 (1:1000)
Phospho-Akt substrate (AGC-family kinase) AB_331810	Cell Signaling Technology, Danvers, MA	#9614	RXXS/T-P	Rabmab IgG	Detects peptides and proteins containing a phosphor-Ser/Thr residue preceded by arginine at the − 3 position	1:1000 (1:500)
Phospho-PKA substrate AB_331817	Cell Signaling Technology, Danvers, MA	#9624	RRXS/T-P	Rabmab IgG	Detects peptides and proteins containing a phosphor-Ser/Thr residue with arginine at the − 3, and − 2 positions	1:1000 (1:500)
PKG substrate (activated) AB_1006404	Acris, Herford, Germany	AM00111PU-N	RKVpSK	Monoclonal Mouse IgG1	Detects peptides and proteins containing the phosphorylated target sequence of PKG	1:500
S-nitrosocysteine AB_10697568	Abcam, Cambridge, UK	ab94930	S-nitrosocysteine conjugated to BSA	Monoclonal Mouse IgG1	Detect nitrosylated cystein moieties	1:1000 (1:1000)
β-tubulin (loading control) AB_1929036	Acris, Herford, Germany	AP15841PU-S	Synthetic peptide derived from aa 416–430 of human β-tubulin	Polyclonal rabbit IgG	Wide specificity in the animal kingdom	1:2000
uNOS AB_260751	Sigma-Aldrich, Saint Louis, MO	N-217	Synthetic peptide (DQKRYHEDIFG), derived from the amino acid sequence 1113–1122 of the N-terminal of the mammalian NOS	Polyclonal rabbit IgG	72% homology with the *Ambigolimax valentianus* (*Lim*NOS, AB333805.1, [73]) consensus sequence (DTNRFHEDIFG). Previously characterized in *Helix pomatia* [27]	(1:2000)
cGMP AB_2314152	Dr. J. de Vente Dept. Psychiatry and Neuropsychology, EURON, Maastricht University, Maastricht, The Netherlands		cGMP-formaldehyde-bovine thyroglobulin	Sheep	Species independent [71]	(1:20.000)

ecular weight (mw) was close to the homologue mammalian protein; and if the immunohistochemical (IHC) localization of the antibody corresponded to the predicted function of the target protein.

2.5. Immunocytochemistry and histochemistry

For studying the relation of cGMP and sGC distribution to NOS by immunocytochemistry, cell suspension of eight PCs obtained from four animals were prepared in HPS, similar to that described in Section 2.2. The cells were spread on a poly-L-lysine coated coverslips placed in a cell culture plate, let to attach by sedimentation for 1 h at room temperature, and subsequently fixed in 4% (w/v) freshly prepared paraformaldehyde (PFA) solution (PFA dissolved in 0.1 M PBS, pH 7.4). For tissue localization of target proteins, dissected cerebral ganglia were fixed also in 4% PFA at 4 °C overnight. Alternatively, in case of S-nitrosocystein IHC, PFA was replaced by 2% glutaraldehyde, as recommended by the antibody producer. After cryoprotection, the specimen was immersed into 20% (w/v) sucrose diluted in PBS for 4 h, then 15 μm frozen sections were cut in a cryostat. In order to enhance cGMP detection in the cells and the tissue, prior to fixation, freshly frozen cell suspensions and cryostat sections were incubated in PBS containing 1 mM SNP and IBMX (Sigma-Aldrich, cat. # 71778; I5879) in darkness for 15 min. If a HRP-based developing procedure was applied, the endogen peroxidase activity was blocked by 1% H_2O_2 in PBS after fixation. Thereafter, non-specific binding sites were blocked by a 1 h long incubation with 4% normal goat (Dako cat. # X0907), or donkey serum (Sigma-Aldrich, cat. # D9663) serum, diluted in PBS containing 0.25% w/v BSA and 0.1% v/v Triton-X 100 (PBS-BSA-TX). Preparations were incubated with primary antibodies (see Table 1) at 4 °C overnight, and then labeled with one of the corresponding secondary antibodies (see Table 2). Both primary and secondary antisera were diluted in PBS-BSA-TX. The biotinylated antibody was labeled with avidin-HRP (1:100, 2 h, constituent of the VECTASTAIN Elite ABC peroxidase kit, Vector Lab., cat. # PK-6200). Between each incubation steps the preparations were thoroughly washed with PBS. HRP conjugated immunocomplex was developed in 0.05% 3,3′-diaminobenzidine (DAB, Sigma-Aldrich, cat. # D5637) and 0.001% H_2O_2, diluted in 0.05 M Tris-HCl, pH 7.6. In case of S-nitrosylation, labeling DAB was enhanced with 0.05% nickel ammonium sulfate (Sigma-Aldrich, cat. # A1827). DAB and Ni/DAB reaction was examined under natural light, whereas the fluorochrome under UV light using the 557/576 nm exci-

Table 2

Antibody name and ID	Producer	Product number	Target primary antibody	Applied concentration in WB (and in IHC)
Rabbit anti-goat ab conjugated with horseradish peroxidase AB_2617143	Dako, Agilent Tech. Santa Clara, CA	P0449	Anti-NMDAζ1 Anti-GCS-β-1	1:2000 (1:2000)
Goat anti-rabbit ab conjugated with horseradish peroxidase AB_2336198	Vector Lab. Peterborough, UK	PI-1000	Anti-PKG-1 Anti-phospho-Akt Substrate (AGC-family kinase) Anti-phospho-PKA Substrate Anti-β–tubulin Anti-uNOS	1:5000 (5000)
Horse anti-mouse ab conjugated with horseradish peroxidase AB_2336177	Vector Lab. Peterborough, UK	PI-2000	Anti-PKG substrate (activated) Anti-S-nitrosocysteine	1:5000 (1:5000)
Donkey anti-rabbit ab conjugated with NL-557 AB_663767	R&D, Minneapolis, MN	NL004	Anti-uNOS Anti-phospho-Akt Substrate (AGC-family kinase) Anti-phospho-PKA Substrate	(1:100)

tation/emission filter combinations. Co-existence of sGC or cGMP with NOS in PC cell smear was studied in double-labeling experiments, in which rabbit anti-uNOS was labeled first with goat anti-rabbit conjugated fluorochrome, followed by labeling goat anti-sGC or sheep anti-cGMP with HRP conjugated rabbit anti-goat, and rabbit anti-sheep secondary antibodies, respectively, and finally by development with DAB and H_2O_2. Immunopositive cells were counted in smears obtained from four pairs of PCs (total number of cells counted were 325) in a light microscope at a magnification of 200 ×.

2.6. cGMP ELISA

cGMP in PC was quantified by a competitive ELISA kit (Cayman Chemical Co cat. # 581021, Tallinn, Estonia) after acetylation. Here only a brief description of the protocol is given, details can be found in the manufacture's guide (http://www.caymaneurope.com/pdfs/581021.pdf, accessed: 12.05.2011). Ten PCs from 5 animals were isolated and exposed to the following chemical substances: 0.2 mM PAPANONOate (NO-donor, Cayman Co. cat. # 82140), 10 μM YC-1 (synthetic molecule which increases sGC activity independent from NO, Cayman Co. cat. # 81560), or 10 μM L-Glu in dark for 15 min. PCs were immediately frozen on iron plate in a − 80 °C freezer. PCs obtained from animals tested previously in behavioral experiments (see below) were dissected, then also quickly frozen, and processed for cGMP measurement. Proteins were extracted by 5% TCA during homogenization the sample on ice. Then TCA was removed by water-saturated ether, and the ether was carefully evaporated by gentle heating. To the sample and kit standards 1/5 volume of 4 M KOH and 1/20 volume of acetic anhydride were added. Samples in two dilutions and three replicates as well as standards were mixed with cGMP acetylcholine esterase tracer and cGMP ELISA antiserum in a 1:1 volume ratio and incubated at 4 °C for 18 h. After rinsing the plate wells with wash buffer the reaction was developed by adding 200 μl Ellman's reagent to each well and incubated the plate at 4 °C for 2 h. Absorbance was read at 405 nm in a microplate reader (Victor[3], Perkin-Elmer, Waltham, MA). cGMP amount was calculated from the binding/specific maximum binding ratio and based on standard calibration.

2.7. Behavioral experiments

To study odor elicited molecular changes, the food finding and appetitive behavioral experimental protocols, described previously for the snail, *Helix pomatia* [69,70], respectively, were followed. Adult animals were collected in the surrounding areas of the institute, kept under laboratory conditions, and fed on lettuce. The animals were motivated by one week starvation, then activated by gentle tap water sprinkling, and placed on a cleaned, standard white plastic laboratory bench surface located in that part of the laboratory where airflow was low. Air currents were minimized during the experiments. The area was free of directional cues and the surface was cleaned from mucus trails, to minimize the influence on the snail's movements, apart from the experimental odorant stimulus. When the animal recovered from the displacement, fresh cucumber slices, as appetitive stimulus, were placed on the surface perpendicular to the animal movement at 15 cm distance. If the snail orientated, and consistently moved towards the odor source, in the open field, and also when the characteristic twitching and quivering behavior appeared, it was considered as a "smelling animal". Those snails that reached the cucumber and started to eat it were considered as "eating animals". As an aversive odor source, grinded garlic pieces were placed 15 cm ahead of the snails' route, animals showing typical aversive behavior were used for experiments. With some of the snails that smelled or ate the cucumber, the behavioral experiment was repeated again after three days. These snails were separated into "smelling after three days" and "eating after three days" groups. As a minimum of 25 individuals were tested in each group. Snails, that failed to display the expected behavior in the test, i.e. moved in random directions, or were not motivated, were excluded from the experiment. Control, naïve snails were active, and were treated identically to animals involved in the experiment, but not exposed to appetitive /aversive stimuli. PCs from behaviorally tested animals were processed for cGMP measurement and protein phosphorylation assay.

2.8. Statistical analysis

Quantitative data were expressed as mean ± S.E. The significance of the difference between means was analyzed by the least significant difference test of analysis of variance (ANOVA). p values < 0.05 were considered as significant.

3. Results

3.1. NO production in PC cells

The PC NO content estimated from the NO_x metabolite concentration of the PC lysate detected by a Sievers NO analyzer was 0.45 ± 0.08 pmol/mg protein.

The characteristics of NO production were investigated using the DAF-2-DA fluorescent NO scavenger (Fig. 1). The specificity of DAF-2-DA fluorescence labeling of intracellular NO was tested in PC cells (Fig. 1A8). In DAF-2-DA free medium neither the HPS itself, nor the suspension of isolated PC cells, showed a fluorescent signal that exceeded the background intensity. When 10 μM DAF-2-DA was added to the HPS the fluorescent intensity increased slightly but not significantly, whereas it became five times higher when PC cells were also present in the DAF-2-DA containing medium.

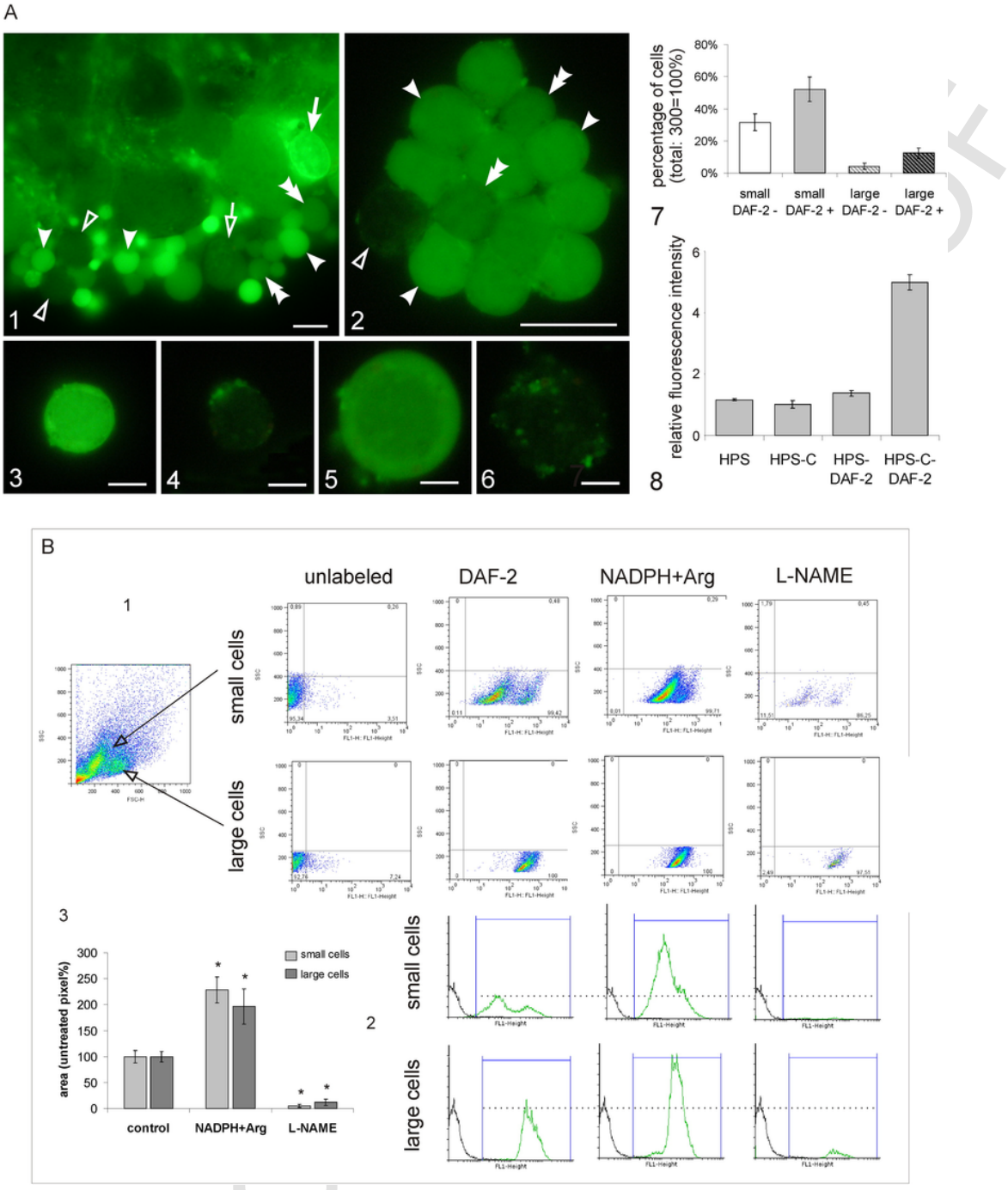

Two populations of PC cells with different perikaryonal size (small neurons: 5–8 μm, larger neurons: 12–15 μm) were distinguished by DAF-2 in the fluorescence microscope (Fig. 1A). They were randomly distributed in the cellular mass of the PC (Fig. 1A1), and DAF-2 fluorescence observed in their cytoplasm, displayed different degrees of staining intensity (Fig. 1A1, 2). > 80% of the PC cells had a small (5–8 μm) perikaryon, out of them about 65% was DAF-2 positive (Fig. 1A3, 4, 7; N_{cell} = 300; N_{PC} = 6 from 3 ind.). Similarly, the majority (70%) of the larger (10–15 μm) neurons, representing 18% of the total PC cell population, also possessed DAF-2 positivity (Fig. 1A5, 6, 7; N_{cell} = 300; N_{PC} = 6 from 3 ind.).

Based on size, isolated PC cells sorted by flow cytometry could also be separated into two populations, small and larger cells (Fig. 1B1). As a result of DAF-2-DA incubation, the fluorescent intensity of the entire cell suspension was enhanced (Fig. 1B1). Small cells could further be divided into subgroups, showing moderate or high fluorescence intensity (Fig. 1B1). Number of DAF-2 positive small cells displaying moderately enhanced fluorescence intensity was threefold higher than those with high intensity. In the case of both small and large cells the number of DAF-2 positive cells increased by 90–130% in the presence of a NOS co-factor mixture (including 1 mM NADPH), and decreased to 5–15% of the total population when the NOS inhibitor 100 μM L-NAME was applied (Fig. 1B1, 2, 3). NOS cofactor mixture also increased the fluorescence intensity of moderately fluorescing small cells (Fig. 1B1, 2, 3). Intensity of DAF-

2 fluorescence in intensely labeled small and large cells remained unchanged after stimulation with the co-factor mixture.

3.2. Involvement of Glu and NMDA in NO release from PC cells

Flow cytometric analysis of PC cells showed that application of both 10 μM Glu and 10 μM NMDA increased the number of small size cells displaying moderate DAF-2 fluorescence by 210% and 186%, and of the larger cells by 64%, and 69%, respectively, compared to control (100 ± 9%, 100 ± 19%; Fig 2A). In addition, the fluorescence intensity of moderately DAF-2 positive small cells was also increased after Glu or NMDA application (Fig. 2A1). In contrast, 10 μM ACh influenced only slightly, or not all, the number and fluorescent intensity of DAF-2 positive neurons. If Glu and NMDA were applied together in 1:1 M ratio no additive effect was observed. In another series of experiments, NMDA-receptor blockade by MK-801 (100 μM), prevented the effect of 10 μM NMDA, and 10 μM Glu, respectively, in small cells, but not in larger ones. In addition, application of MK-801 alone decreased the number of DAF-2 positive small cells, but had no effect on the larger ones.

In *Helix pomatia* CNS protein extract a moderate single band was detected, around 130 kDa mw by Western blot when the blot membrane was probed with a polyclonal anti-NMDARζ1 antibody (Fig. 2B). In *Lymnaea stagnalis* extract, used as a positive control, for the NMDA-receptor sequence [46], anti-NMDARζ1 detected a strongly labeled double band at the same mw. Probing *Helix pomatia* CNS protein extracts with NGS revealed that the other immunoreactive bands arose due to non-specific binding

Immunohistochemical localization of the NMDAR-like protein in the PC (Fig. 2C) was highly similar to that of NOS [27,28]. Interperikaryonal trajectories within the cell mass, the lateral regions of the terminal neuropil area, and the internal neuropil, were labeled by the anti-NMDARζ1 antibody (Fig. 2C1). At higher magnifications (Fig. 2C2) NMDAR-like immunoreactive (IR) elements were found in PC cell perikarya, being located more frequently at the distal margin of the PC. Immunoreaction was intensively labeled in the external region, perhaps representing the cell membrane of these cells. Beside the PC, discrete meso- and metacerebral elements were also detected by the anti-NMDARζ1 antibody (Fig. 2C1).

3.3. NO-induced cGMP in the PC

Using a mammalian sGC antibody with 100% epitope homology to the sGC sequence identified in *Lymnaea stagnalis* (see Table 1.), a 65 kDa mw protein was detected by Western blot in the *Helix pomatia* PC protein extract (Fig. 3A). The mw of this protein was identical with that of the mammalian sGC.

The sGC antibody labeled heterogeneously the terminal and internal neuropils and some perikarya of globuli cells in close location to the distal border of the PC, at the proximal part of the cell mass, and in front of the internal neuropil (Fig. 3B1, 2). Intercellular spaces among globuli cell perikarya also showed sGC-like immunoreactivity (Fig. 3B1). When freshly prepared unfixed PCs were stimulated by incubation in a mixture of 1 mM SNP and IBMX, cGMP immunoreactivity could be localized in the internal neuropil and the terminal neuropil which was also faintly labeled by the anti-cGMP antibody (Fig. 3B3). cGMP immunolabeling was also seen in the cytoplasm of globuli cells, more frequently in those situated near to the distal margin of the cellular mass (Fig. 3B4). After stimulation of the PC cell suspension with 1 mM SNP/IBMX mixture, cGMP immune-signal from PC cell smears showed that 15% of the 'small', and 8% of 'larger' cell types were cGMP positive (Fig. 3B 8, 9). Double-labeling of the PC cell smears with NOS and sGC/cGMP antibodies revealed that most of the sGC-like IR (Fig. 3B6) and cGMP-IR (Fig. 3B8) cells also revealed NOS-immunoreactivity (Fig. 3B5, 7, B10). In addition, among the small NOS positive cells, 80% showed cGMP immunoreactivity (Fig. 3B10). On the other hand 69% of the small cells, and 50% of the larger cells, proved to be immunonegative both for NOS and cGMP (Fig. 3B 7, 8, 10).

sGC activity of PC cells, hence their cGMP production, was revealed by cGMP EIA in the presence of 10 μM YC-1, an NO-independent sGC stimulator, and 0.2 mM PAPANONOate, a NO-donor (Fig 3C). The first treatment stimulated cGMP synthesis by 2.25 fold and the latter by 1.5 fold. Incubation of the PC cell suspension with 10 μM Glu elevated the cGMP level by 2.5 fold.

3.4. NO-(cGMP) target molecules in the PC

Western blot of the PC extract probed with an anti-PKG-1 antibody showed a single band around 74 kDa mw, which is close to the mw of the mammalian PKG-1 (78 kDa, Fig. 4A1). This band was also detected beside another lower mw protein by the antibody recognizing the phosphorylated target sequence of PKG-1. When isolated PCs were exposed to 1 mM SNP ex vivo, the PKG-1-like IR band was detected at around twice the mw as in case of unstimulated conditions. PKG-1-like immunoreactivity was prominent in the lateral and intermediate neuropils, with intense signal also seen along the lateral edge of the terminal neuropil (Fig. 4A2) where afferent fibers enter from the direction of the tentacular ganglion, and efferent fibers innervating the tentacular muscles leave [10]. In the labeled intermediate and lateral neuropils the anti-PKG-1 antibody revealed a dense,

Fig. 1. NO visualization by DAF-2 in PC neurons. A. Fluorescence microscopic view of NO producing neurons. DAF-2-DA labeled whole-mount PC preparation (A1) and isolated PC cells (A2–6). NO positive small cells with high (A3 and arrowheads in A1, A2) or moderate (double arrowheads in A1, A2) intensity; NO negative small cells (A4 and open arrowheads in A1, A2); NO positive large cells (A5 and arrow in A1); NO negative large cells (A6 and open arrow in A1). Scale bars: 10 μm in 1, 2; 5 μm in 3–6. A7. Percentage of small and large neurons present in the PC cell smear and possessing or lacking NO activity. $N_{cell} = 300$; $N_{PC} = 6$ from 3 individuals. A8. Specificity control of DAF-2 intracellular labeling. HPS: *Helix pomatia* physiological saline, C: PC cells. HPS and HPS-C media were incubated with or without 10 μM DAF-2-DA for 15 min, then fluorescence intensity was measured at 485/600 ex/em filters in a microplate reader. B. Flow cytometry of isolated DAF-2-DA labeled PC neurons. B1. Representative registrations of cell flows, DAF-2 fluorescence of cells, and its change after incubation with NOS cofactor mix (1 μM NADPH, arginine) or 100 μM L-NAME, for 15 min. Unlabeled cells are shown in size (abscissa) - autofluorescence intensity (ordinate) relation. DAF-2 labeled cells are shown in fluorescent intensity (abscissa) – size (ordinate) relation. Different colors symbolize the amount of particles. The wavelength of the color increases with the number of particles. Minimum number of cells counted was 20×10^5, which was obtained from 6 PCs of 6 animals. The position of unlabeled cells is indicated by rectangle lines. As the result of DAF-2-DA incubation, the location of the cell populations shifted right along the horizontal axis in the plot. NOS cofactor mixture increased the number of PC cells, indicated by the enhanced area of intensive color, and also the fluorescent intensity of moderately fluorescing small cells, indicated by the right shift of this subgroup, and hence decreasing distance between the location of the moderately and intensely DAF-2 positive cells in the plot. B2. Histograms of the cell number at different fluorescence intensities. Blue rectangles covering the green color histograms show the effect of treatment. Black color histograms: unlabeled cells. Dashed line: maximum number of DAF-2 positive cells in control experiment. B3. Percentage of DAF-2 positive cells (mean ± S.E.) after incubation with the cofactor mix (10 μM NADPH + Arg) or 100 μM L-NAME. DAF-2 positive cells are control (small cells: 100 ± 12%, large cells: 100 ± 10%). Both treatments significantly change the cell number of small as well as large cells compared to their own controls. N = 5. ANOVA, $*p < 0.05$. (For interpretation of the references to color in this figure legend, the reader is referred to the web version of this article.)

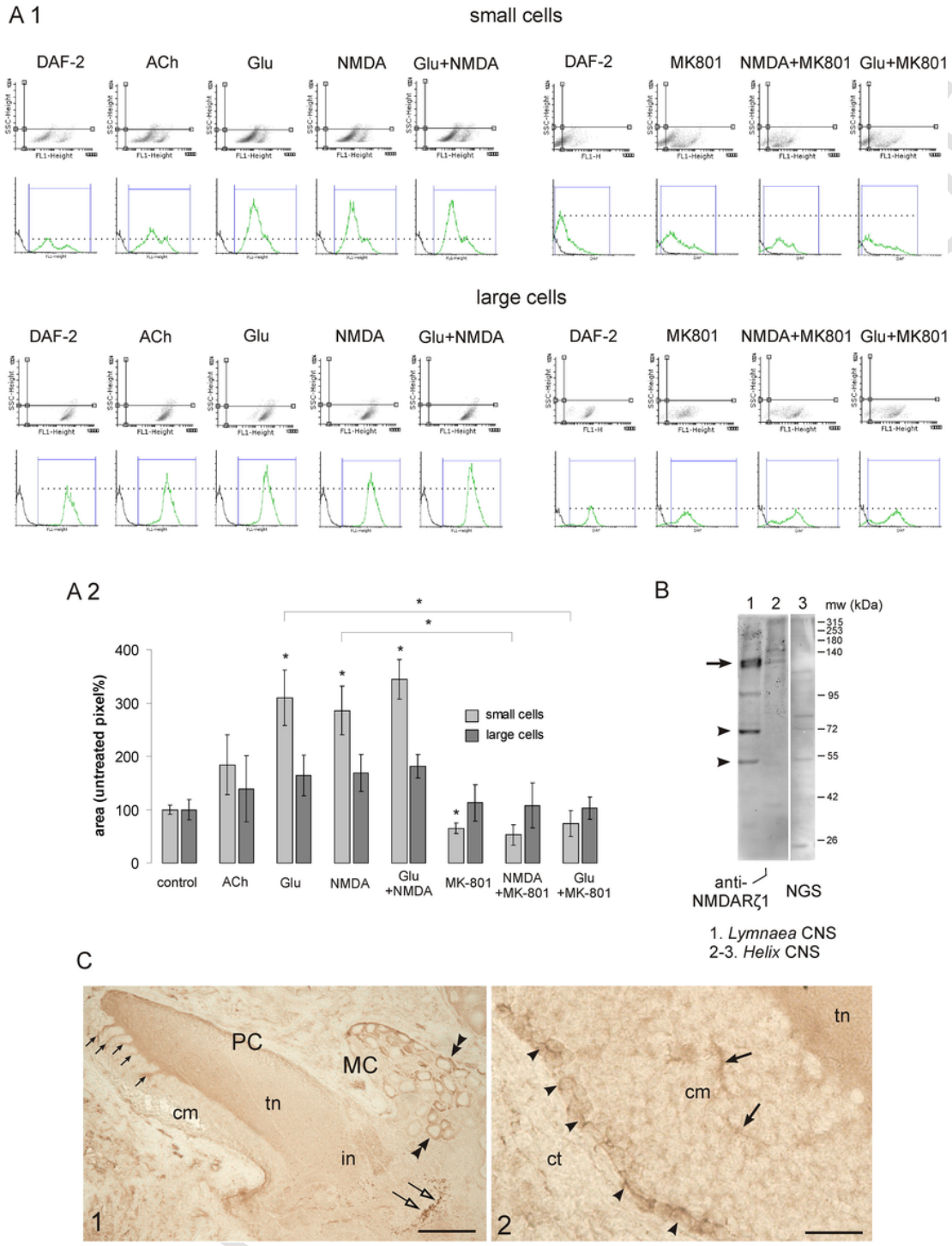

fine network, of projections (Fig. 4A2). Subpopulation of PC cells at the bottom of the cellular mass showed PKG-1-like immunoreactivity (Fig. 4A3). However, PKG-1-like immunoreactivity was absent in most parts of the cellular mass, and from the terminal and internal neuropils (Fig. 4 A2). The antibody recognizing phosphorylated residues of PKG-substrates failed to function in immunohistochemical application (the producer did not recommend this kind of application either).

PC protein extract probed with the phospho-AGC kinase substrate (AGC-S-P) antibody labeled different proteins, including 28, 45 and 55 kDa mw bands, whose immunoreactivity was enhanced following incubation in a mixture containing the NO-donor 1 mM SNP and the phosphodiesterase inhibitor, IBMX (Fig. 4B1). Another NO-donor, SNAP, and IBMX alone, or in combination with the adenylate-cyclase activator forskolin (1 mM), exerted the same effect on the 28 and 45 kDa proteins. In contrast, treatments that influenced the cyclic nucleotide level in the PC did not change the intensity of labeling of the higher mw protein bands (97, 150 kDa mw) recognized by the AGC-S-P antibody. Forskolin did not change phosphorylation of the 55 kDa protein, but did decrease the level of AGC-kinase dependent

phosphorylation of the 80 kDa protein, effects which were not seen with a DMSO control, or NO-donor treatment. In addition, SNP did not influence the intensity of the tubulin-IR band used as a loading control. Immunohistochemical studies showed that immunoreactivity for the AGC-S-P was present in the whole PC tissue with enhanced signal intensity in the terminal and internal neuropils (Fig. 4B2). In the cell mass, strong AGC-S-P immunoreactivity was observed in PC cell perikarya and axon bundles projecting between them towards the terminal neuropil (Fig. 4B3). Proteins displaying marked phosphorylation by AGC kinase were also immunoreactive against the antibody raised to PKA phosphorylated substrate (PKA-S-P) (Fig. 4B1), and a similar distribution pattern and intensity of PKA-S-P immunoreactivity was observed to that found in anti-AGC-S-P labeled PC sections (Fig. 4 B4–5).

Incubation of PC pieces with 1 mM GSNO, the natural NO source and trans-nitrosylation agent, resulted in increased protein S-nitrosylation in a number of proteins, one of them possibly corresponding to the 55 kDa mw tubulin (Fig. 4C1). With an antibody labeling S-nitroso-groups distal parts of the cell mass, as well as the internal and intermediate neuropils were detected by immunohistochemistry (Fig. 4C2). At higher magnification it appeared that the immunoprecipitation surrounded PC cells and filled up the interperikaryonal space (Fig. 4C3, 4).

3.5. Odor elicited cGMP and AGC kinase dependent protein phosphorylation in the PC

In order to reveal the involvement of NO and putative members of the NO-induced molecular cascade in odor sensing, PC cGMP levels, and protein phosphorylation by the AGC family kinases, were followed during food discovery behaviors (Fig. 5). Subsequent events of perceiving, finding, tasting and eating the food were indicated by different, well separated body postures of the snail, and especially by the position of the tentacles (Fig. 5A1–4) [69,70]. In particular, when in the active (motivated) state, the snail's body was fully extended, with the animal crawling with tentacles erected upward, screening the environment (Fig. 5A1). When the appetitive odor of the cucumber was perceived the animal turned towards the food (Fig. 5A2) and oriented both tentacles stiffly towards the food (Fig. 5A3). Reaching the food source, the tentacles became shortened, were bent down, and the feeding movement of the buccal apparatus commenced (Fig. 5A4). In contrast, when an unpleasant/aversive smell source, such as garlic, was placed in the front of the snail, the animal made numerous twitching motions with the tentacles, before these were then shortened, and the animal recoiled, withdrew into the shell (Fig. 5A5), and finally ejected mucus.

cGMP levels in the PC of odor (cucumber) stimulated snails was twice as much (205 ± 25%) as that measured from the PC of control animals (100 ± 18%, 26.5 ± 4.8 pmol/ml, N = 10), not exposed to odor stimulus (Fig. 5B). In snails that had already started eating the cGMP level increased less, being 149 ± 15% of the control level. In contrast to cucumber exposure, presentation of garlic resulted in a significant reduction (19 ± 4%) of the cGMP level compared to controls.

Western blot of AGC kinase phosphorylated proteins extracted from the PC showed that four proteins ranging between the 40–60 kDa mw were intensively labeled regardless of the state of the odor-elicited behavior (Fig. 5C1). Analysis of these proteins revealed similar intensities of immunoreaction both within each snail, and between the experimental groups. In the PC of smelling and eating snails AGC kinase induced phosphorylation of a 28 kDa protein in 75% (15 snails) and 50% (10 snails), respectively, of the tested animals (20 in total) (Fig. 5C1, 2). However, when the animals were exposed again to the odor stimulus three days after the first encounter, an enhanced phosphorylation of the 28 kDa protein was detected in the PC of only 20% (4 snails) at the smelling state, while none of them showed enhanced phosphorylation when the snail started eating. In those smelling snails that possessed enhanced phosphorylation of the 28 kDa protein, three other bands. > 100 kDa mw also showed hyperphosphorylation (Fig. 5C1). Garlic exposure, however, did not promote phosphorylation of these proteins.

4. Discussion

4.1. NO-producing cells in the PC

We used the Sievers NO-analyzer to measure levels of NO in from the PC of *Helix pomatia*. These NO measurements fall within the same order of magnitude previously obtained from extracellular NO electrodes in *Limax* sp. PC [41,72]. These observations, taken together with the findings of other authors [26,40,41,69] and our recent data [27,28] indicate that NO is a prominent neurochemical substance in the olfactory center of terrestrial snails. Applying NO-scavenger, fluorescence microscopy, and flow cytometry, we have provided further evidence that both the NB and B cell types of isolated PC neurons [1] are capable of synthesizing NO. This was also proved earlier in *Limax* sp. by in situ hybridization of *lim*NOS1 mRNA in the PC, and by RT-PCR from separated PC cells [42]. The novelty of our findings is that NB cells can be further subdivided into two populations containing different amounts of NO. When isolated PC cell perikarya were stimulated with the NOS co-factor mixture, or the putative NOS activator Glu and NMDA, the number of moderately NO-fluorescing NB cells and their NO production (DAF-2-DA fluorescence) increased. In contrast, only the number, but not the fluorescence of the intensely fluorescing NB cells and B cells, changed after the same stimuli. Although NO production increased in moderately fluorescing NB cells following different stimuli, yet their fluorescent

Fig. 2. Glu mediates NO synthesis in the PC possibly through NMDA-receptor activation. A. Flow cytometry of isolated DAF-2-DA (0.5 μM) labeled PC neurons. A1. Representative registrations and histograms of DAF-2 positive cell types after incubation with 10 μM ACh, 10 μM Glu, 10 μM NMDA, a 1:1 mixture of 10 μM Glu and 10 μM NMDA, 10 μM MK-801, and mixtures of 10 μM NMDA + 10 μM MK-801, and 10 μM Glu + 10 μM MK-801. The position of unlabeled cells is indicated by rectangle lines. Blue rectangles covering the green color histograms show the effect of treatment. Black color histograms: unlabeled cells. Dashed line: maximum number of DAF-2 positive cells in control experiment. The increased number of DAF-2 positive PC cells, indicated by the density of the cell populations, and the enhanced fluorescence intensity of moderately DAF-2 positive small cells indicated by the right shift of the location of this cell population, and hence decreasing distance between the moderately and intensely fluorescing populations in the plot, are seen after Glu or NMDA exposition. A2. Quantitative analysis of flow cytometry data. Data are given as percentage of DAF-2 positive cell number (mean ± S.E.), where non-treated DAF-2 positive cells were the control (small cells: 100 ± 9%, large cells: 100 ± 19%). Significant differences between control and experimental bars, and connected bars are labeled. N = 5. ANOVA, $*p < 0.05$. B. Immunoblot demonstration of a NMDA-receptor-like protein (arrow) in the CNS extracts of *Lymnaea stagnalis* (B1) and *Helix pomatia* (B2–3). Arrowheads: unspecific bands. B3. Control, non-immunized purified normal rabbit serum (NRS) is used as a primary antibody. C. Immunohistochemical demonstration of the anti-NMDAζ1 receptor antibody labeled structures in the PC at lower (C1) and higher (C2) magnifications. Note uniform labeling of low intensity in the terminal (tn) and internal (in) neuropils in C1 and the labeled axon trajectories (in C1 small and in C2 regular arrows) throughout the cell mass (cm) layer. Arrowheads indicate labeled neural perikarya at the distal PC region. Note also numerous labeled cells (double arrowheads) in the mesocerebrum (MC) and varicose axons in the metacerebrum (open arrows). ct: connective tissue. Scale bars: 100 μm in C1; 25 μm in C2. (For interpretation of the references to color in this figure legend, the reader is referred to the web version of this article.)

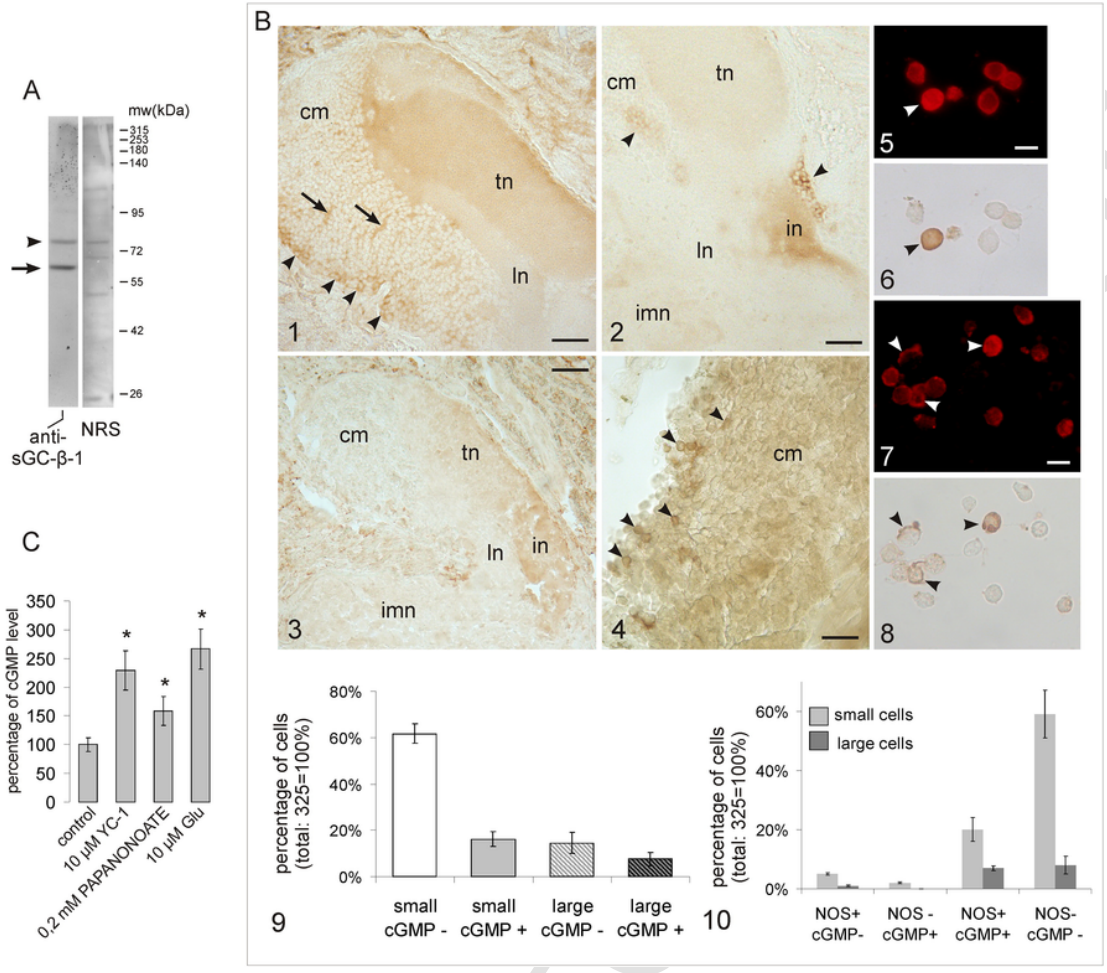

Fig. 3. cGMP in the PC. A. Immunoblot demonstration of a sGC-like protein (arrow) in the CNS extract. NRS: membrane probed with a non-immune normal rabbit serum. Arrowhead: non-specific band appearing in both membrane strips. B. Immunohistochemical demonstration of anti-sGC antibody (B1, B2, B6), and anti-cGMP antibody (B3, B4, B8), respectively, labeled structures. B1–4. PC tissue sections. Arrowheads: immunoreactive perikarya in the cell mass (cm) layer; arrows: sGC-IR trajectories in the cm. Note heterogeneous labeling in the terminal (tn) and internal (in) neuropil. ln: lateral neuropil; imn: intermediate neuropil. B5–8. Paired microphotographs (B5–6, B7–8) showing double-labeling (arrowheads) of isolated PC cells with anti-NOS immunofluorescence (B5, B7) and anti-sGC (B6), or anti-cGMP (B8) immunoperoxidase techniques. Scale bars: 100 μm in B1–3; 25 μm in B4; 10 μm in B5–8. B9–10. Quantitative analysis of isolated PC cells showing cGMP immunoreactivity alone (B9) or co-labeled with anti-NOS antibody (B10). Data are presented as percentage (mean ± S.E.) of total cells counted (100% = 325) obtained from 4 preparations (N = 4, 8 PCs). C. cGMP content of isolated PC cells after incubation the cell suspension with the NO-independent sGC stimulator YC-1, the NO-donor PAPANONOATE, and Glu. cGMP EIA assay. Control: cGMP concentration of untreated cells (= 100%; 38.2 ± 4.2 pmol/ml; N = 5 preparations, 10 PCs). ANOVA, *p < 0.05.

intensity failed to reach the level of intensely fluorescing cells, suggesting that both cell types possess discrete NO synthesizing properties. This is also supported by the observation that silent cells could start to produce NO after stimulation, hence the number of NO producing cells can increase within NB cell subtypes, while the NO level remained different between the two subtypes. Recently, a new NOS gene, *lim*NOS2, was sequenced from the *Limax valentianus* genome, and found to be present exclusively in a large number of PC neurons, the majority of which were NB cells [43]. Consequently, both *lim*NOS genes are active in PC cells, and both have several regulatory sites [43,73], suggesting a complex level of regulation capable of allowing different levels of NO synthesis. We hypothesize that these two isoforms are responsible for the two characteristically different levels of NO production in *Helix pomatia* NB cells. We also assume that NO production may be constitutive (and possibly saturated) in NB cells intensely producing NO, whereas it can be induced in moderately fluorescing ones. In vertebrates, two constitutive and one inducible forms of the NOS gene have been described. In contrast, there are only a few invertebrate species, in which more than one NOS isoform has been sequenced, and in these few cases the function of the homologues have not been clearly determined [53]. In this context, the functional significance of the two NB cell populations producing different amount of NO is difficult to explain. Possibly, differences in NO production arise through distinct regulatory mechanisms, and serve different functions. A similar situation has already been described in the pond snail, *Lymnaea stagnalis*, where permanent NO levels are critical at the beginning of memory acquisition, and an elevated NO level, generated by *Lym*NOS1 gene expression, is necessary during subsequent phases of memory consolidation [59]. The functional consequences arising from, pharmacological manipulations of NO levels in the PC have been described earlier [26,72]. The former study showed that LFP are mediated by NO through the elevation of B cell bursting frequency, and by ceasing the spiking activity of NB cells through a mechanism involving modulation of the inhibitory input of B cells on NB cells. The latter study demonstrated that inhibition of NO synthesis by L-NAME was also capable of blocking the frequency increase, and enhanced spatial synchronicity,

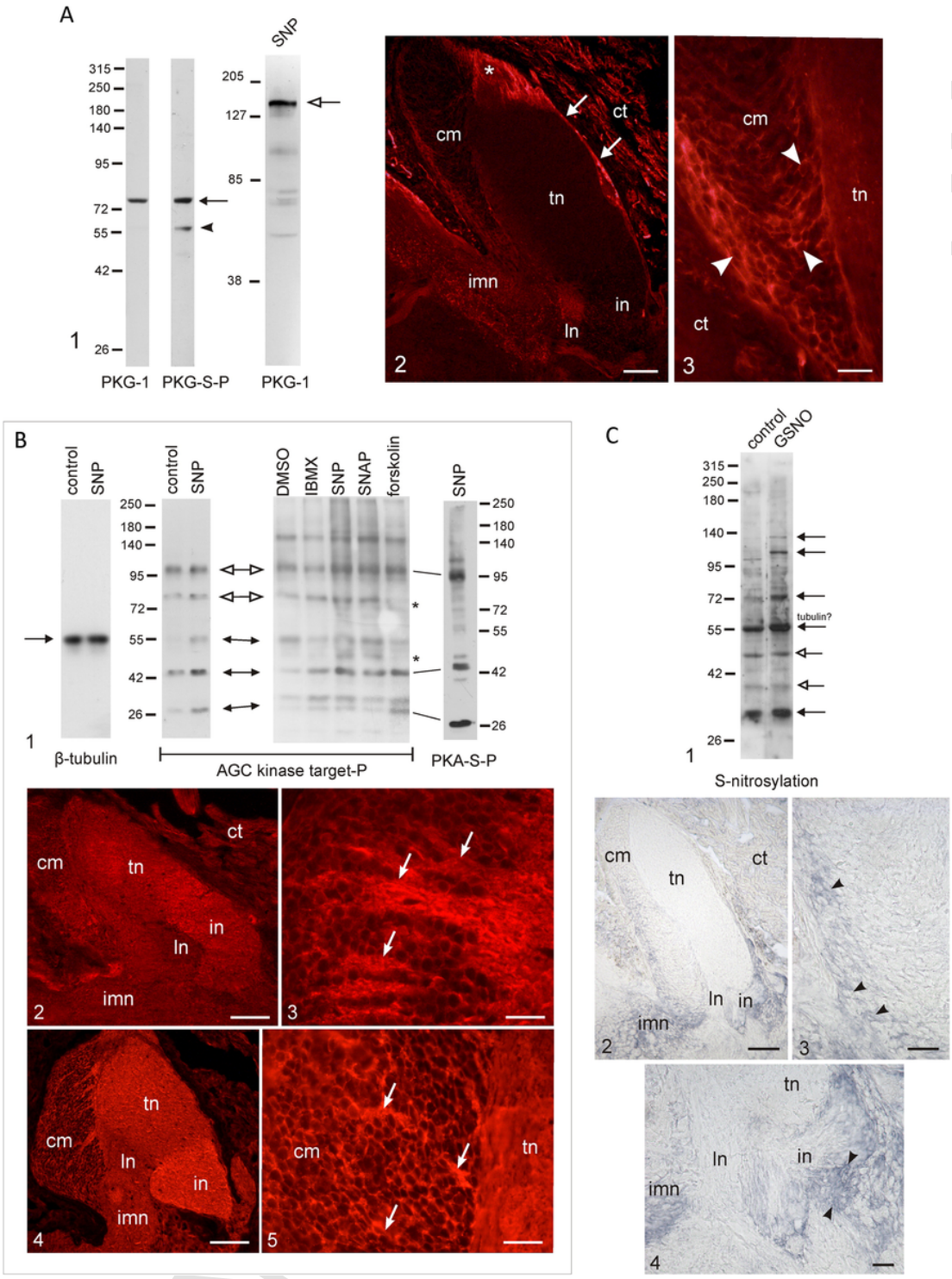

of activity of PC cells during odor exposition in a semi-intact preparation.

4.2. Glu is a potential endogenous inducer of NO synthesis in the PC

According to our results, applications of Glu at low micromolar levels increases both the number of moderately NO synthesizing NB cells, and the production of NO by these cells. This implies that Glu can be an endogenous stimulator of NO synthesis, particularly in a subpopulation of NB cells. The effect of Glu on NO synthesis is less pronounced in both NB cells producing NO intensely, and B cells, suggesting that the regulation of NO synthesis in these cells might be less dependent on Glu signaling. This may be explained if NO production is permanent in these cells, and thus not externally regulated. Alternatively, these cells may not possess sufficient functional GluR to mediate a measurable activation of NO production. Irrespective of the cause, substantial evidence supports our hypothesis that Glu acts to

stimulate NO synthesis. For example, (i) Glu and vGluT immunoreactivity are detected in both PC neuron types [23]; (ii) Glu acts as a negative regulator of NB cell firing via mechanisms involving an inhibitory K^+ channel, and through excitation of B cells via a Cl^- coupled intracellular increase of Ca^{2+} [44]; (iii) the dynamics of Glu release are synchronized and share similar physiological properties with the LFP oscillation [23].

The effect of Glu on the number and activity of moderately NO-producing NB cells could be mimicked by NMDA. Moreover, these effects were sensitive to the NMDA blocker, MK-801, the application of which also diminished the number of this NB cell subpopulation. On the other hand, our experiments suggest that non-NMDA type GluR do not participate in the Glu-evoked response on NO synthesis. First, MK-801 was capable of entirely preventing the effect of Glu, and second, combined application of Glu and NMDA in 1:1 concentration ratio did not result in an additional elevation of NO production in contrast to their single application. Further evidences for NMDA-receptor-mediated NOS activation in NB cells are coming from immunological experiments. First, the mammalian NMDA-receptor antibody revealed an NMDA-receptor-like immunoreactivity in a protein band migrating at the same mw as the mammalian NMDA-receptor ζ subunit (115 kDa), and also at the mw of the putative *Lymnaea stagnalis* NMDA-receptor. However, the intensity of labeling was much lower in *Helix pomatia* than in *Lymnaea stagnalis*, suggesting difference in the epitope regions of the putative NMDA-receptor in the two species. Second, on PC tissue sections the NMDA-receptor-like protein was localized in the same neuronal PC elements (PC cell surface, trajectories projecting towards the terminal and internal neuropils), where the presence of NOS is also prominent [26,27,28,41,42]. Since NB cells, but not B cells, project to the internal neuropil it is assumed that NMDA-receptor-like immunoreactivity belongs to NB cells in the PC. If it is considered that B cells are the main source of Glu [12], then a glutamatergic input that evokes NO synthesis on NB cells seems reasonable (see Fig. 6.). The detection of NMDAR immunoreactivity in the internal neuropil, which receives afferent inputs from the motor centers of the pedal and buccal ganglia [17], suggests a role for NMDA-receptors in nitrergic regulation of the activity of these neurons. However, based on the present study, it is hard to make any suggestion on the interaction of Glu and NO in this structure, since the flow cytometry studies we conducted were limited exclusively to perikarya located in the cell mass.

4.3. Downstream targets of NO in the PC

Both in vitro and in situ NO-induced cGMP synthesis was detected in the PC, in which sGC (β-1 subunit)-like immunoreactivity was also localized. IHC investigations on PC tissue preparations, and double ICC labeling experiments on cell smears, showed that the sites of NO synthesis overlap highly with that of cGMP induction, e.g. they are simultaneously present in a number of NB and B neurons and the internal neuropil. While these findings fit with the earlier observation on the morphological distribution of NOS and cGMP in *Helix pomatia* CNS [66], they contradict the study by Fujie et al. [41], who demonstrated that cGMP accumulates after NO application exclusively in the terminal mass and perikarya that lack NADPH-diaphorase activity. On the other hand, Fujie et al. [42] also found that the mRNA probes of the identified α, β1, and β2 isoforms of the *Lim*sGC both labeled NB and B cell perikarya, suggesting that both cell types are capable of synthetizing cGMP. The latter finding supports our observations, with the slight difference that we found sGC-like and cGMP immunoreactivity, in the internal neuropil, while this structure lacked sGC mRNA and cGMP in *Limax*. Considering that we applied the same methodology and cGMP antibody to localize cGMP synthesis as Fujie et al. [41], we assume that differences exist at the cellular and compartmental levels in the PC of the two, otherwise anatomically and functionally identical systems. The main differences, based on the cGMP localization, between our studies, and those on *Limax* PC [41,42], are that in *Helix pomatia* an intracellular NO-cGMP signaling is likely present in both the cellular mass and the internal neuropil, whereas in *Limax*, an intercellular retrograde transmission of NB cells to B cells in the cell mass, and a cGMP-independent NO action in the internal neuropil is proposed.

The PKG-like-IR band in PC protein extract, and immunoreactive signal in tissue sections, indicate that a cGMP-dependent protein kinase-like protein is present, and might function as a cGMP target in the PC. Detection of a possible PKG dimer in homogenate exposed to an NO-donor suggests that accumulated cGMP promotes the dimerization process of this putative PKG protein and increases its activity. Immunolabeling of the band showing the putative PKG-like protein with the PKG-S-P antibody indicates an auto-phosphorylation process. Both dimerization and auto-phosphorylation are known to augment PKG activity [51]. However, localization of this protein with sGC and cGMP immunoreactivities is restricted to cells located at the base of the cellular mass, suggesting that intracellular coupling of cGMP-PKG is confined to a specific part of the PC. Functionally different cell subpopulations have recently been described in the PC [74], which together with the present findings, indicate that the neurochemical composition of the cell mass may not be uniform. NO-cGMP-PKG signaling may also be involved in processing odor and taste information, since much like the IHC localization of NOS [27,28], PKG-1-like immunoreactivity was found in the intermediate and lateral neuropils, which are located at the border of the pro- and metacerebrum and receive input from the labial nerves [9,27]. Efferent fibers of the olfactory and external peritentacular nerves [10] possessing PKG-like immunoreactivity are located adjacent to the NOS/sGC/cGMP-IR terminal and internal neuropil areas. Labeling intensity

Fig. 4. Putative molecular targets of NO-cGMP signaling in the PC. A. Immunoblot (A1) and immunohistochemical (A2–3) demonstration of a PKG-1-like protein. 1. Arrow: positive band reactive both for the anti-PKG1 and the anti-phospho PKG substrate antibodies. Arrowhead: additional band labeled by the anti-phospho PKG substrate antibody. The anti-PKG1 antibody labels a high mw protein (open arrow), possibly a PKG-1 dimer, when PC was incubated with SNP. A2. PKG-1-like immunoreactivity in the intermediate (imn), lateral (ln) neuropils, and the lateral edge of the PC (arrows). Asterisk: PKG-1-like immunoreactivity at the distal part of the terminal neuropil (tn) where elements of the tentacular nerve (arrows) corresponding to the PC. A3. Enlarged detail of the proximal part of the cellular mass showing PKG-1-like IR neural perikarya (arrowheads). B. Immunoblot (B1) and immunohistochemical (B2–5) evidences for the presence and activity of AGC family protein kinases. B1. Cyclic nucleotide activator induced protein phosphorylation by AGC kinases (double headed arrows) in PC extract. Double headed open arrows: AGC kinase phosphorylated proteins that are not induced by the cyclic nucleotide activators. Arrow: β-tubulin-IR band used as loading control. Identical bands that are intensively IR for both PKA-S-P and AGC-S-P are interconnected with lines. *: proteins that are intensely AGC phosphorylated by SNP and SNAP but not by forskolin. B2–3: AGC-S-P, B4–5: PKA-S-P targets. Note similar structures labeled by both antibodies, and more intensive immunolabeling by the anti-PKA-S-P antibody. Arrows: IR axon trajectories in the cell mass (cm). ct: connective tissue; in: internal neuropil; imn: intermediate neuropil; ln: lateral neuropil; tn: terminal neuropil. C. S-nitrosylation of PC proteins. C1. Level of S-nitrosylation is enhanced by 1 mM GSNO in a number of proteins (arrows). One of them (55 kDa mw labeled protein) possibly corresponds to tubulin. Unchanged levels of S-nitrosylation are indicated by open arrows. C2–4. S-nitrosylated structures in the cell mass (cm), internal (in) and intermediate (imn) neuropils in NO-donor stimulation-free preparations. Arrowheads: immunoreactive material within and surrounding PC cell perikarya. ct: connective tissue; ln: lateral neuropil. Scale bars: 100 μm in A2, B2, B4, C2; 25 μm in B3, B5, C3, C4; 10 μm in A3.

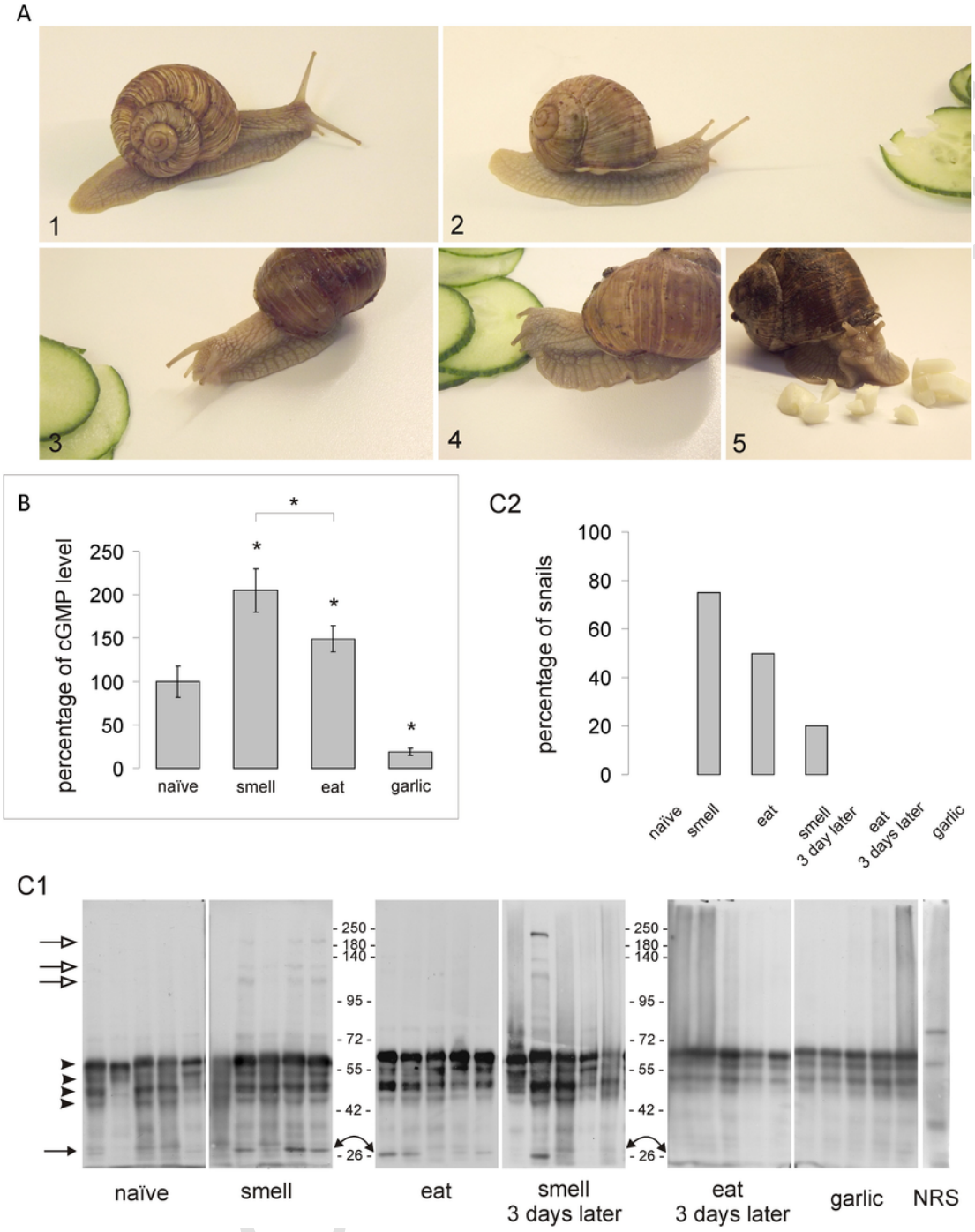

Fig. 5. Changes in the level of possible NO targets in the PC during detection of odor stimulus and feeding. A. Snail postures at (A1) normal, active motion, (A2) perceiving the attractive odor stimulus (cucumber), (A3) reaching the food source, (A4) eating, and (A5) rejecting the unfavorable food (garlic). B. cGMP content of the promptly isolated PCs measured after snails caught the odor of, fed on the cucumber, or were exposed to garlic. cGMP EIA assay. N = 10 (obtained from 5 animals). Control: cGMP concentration of naïve animals (= 100%, 26.5 ± 4.8 pmol/ml). ANOVA, $*p < 0.05$. C. Western blotting of AGC kinase phosphorylation of PC proteins at different behavioral states shown in A (naïve animal: active snail with no food exposition; smelling the attractive odor; eating; rejecting the garlic). Animals exposed again to the odor stimulus three days after the first trial were also tested. C1. Representative blots. Paired PCs obtained from one animal were run in each lane (loaded protein weight: 100 μg). Solid single and double arrows: 28 kDa protein. Arrowheads: AGC-S-P-IR bands which phosphorylation level is permanent, and independent of the behavioral state. Empty arrows: hyperphosphorylated bands in smelling snails. C2. Percentage of snails displaying enhanced phosphorylation of the 28 kDa protein in the course of the subsequent behavioral states (N = 20).

of the cGMP-IR neuropil areas showed a similar pattern to that of NOS [27,28], with a declining gradient from proximal to distal direction, which suggests volume transmission of NO and cGMP in the terminal neuropil. In the PC externally applied cGMP [42] and NO [26] evoked oscillation frequencies in a dose-dependent manner, reminiscent of findings from mammalian CNS where fluctuating extracellular cGMP was shown to follow NO level [75]. Hence it is possible that cGMP acts as an intercellular messenger that, through volumetric

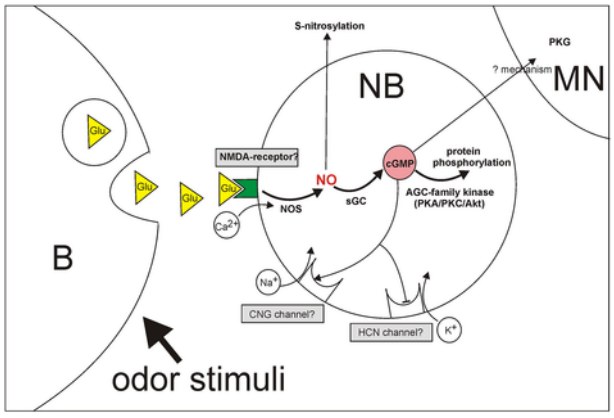

Fig. 6. Suggested scheme of the proposed NO-signaling molecular cascades in *Helix pomatia* PC. Odor stimuli possibly evoke Glu release from B neurons which activates NO production in moderately NO productive (inducible) NB cells through a putative NMDA receptor-like channel. NO induces cGMP synthesis, and the cyclic nucleotide activates some of the members of the AGC family kinases, resulting in protein phosphorylation of specific proteins. Alternatively, cGMP can act as an intercellular messenger initiating PKG activity in motoneurons (MN) innervating tentacle muscles, or influencing bursting properties by regulating CNG or HCN-coupled ion channels in some of the PC cells. The excess of NO might be pooled or neutralized by extracellular proteins through S-nitrosylation. Constitutive NO production by B and highly NO productive NB cells might contribute to the maintenance of the regular firing pattern resulted from the neuronal interaction between these cell types. Identified elements and events of the hypothetic pathway are indicated by bold lettering.

transmission in the PC, modulates tentacle muscle activity via PKG containing effector nerves.

We have no evidence on the intracellular function of cGMP in PC neurons. However, our findings on the location of cGMP and the distribution of the $K_v4.3$ potassium channel in *Helix pomatia* PC [76] suggests that cGMP might act directly on a CNG or a HCN channel as shown in the CNS of *Lymnaea stagnalis* and *Aplysia* sp., where NO/cGMP evoked EPSP by the inhibition of K^+ channels [77,78]. In *Helix pomatia* PC, it also seems likely that cGMP signaling is connected to PKA. In this context, PKA was shown to be synergistically stimulated by both cAMP and cGMP in the olfactory glomeruli of *Apis*, where it played a pivotal role in neuronal events underlying olfactory learning of honeybee [60]. Opposite to the PKG-like labeling, phosphorylated PKA substrate localization in the *Helix pomatia* PC shows a similar map to that of NOS/cGMP, providing morphological evidence for the possible cross-talk between cAMP and cGMP signals. The distribution map of PKA phosphorylated proteins is very similar to that of phosphorylated targets of AGC kinase, implying that common target proteins regulated by members of the AGC-family kinases are present in the PC. Increased phosphorylation events (28, 45 kDa mw proteins) after stimulation of the adenylate cyclase ex vivo with forskolin, and the guanylate cyclase with NO-donors, also suggests a putative cross-talk between cAMP and cGMP induced molecular cascades. On the other hand, proteins showing enhanced phosphorylation due to the application of NO-donors, but not to forskolin (50, 80 kDa mw proteins), indicate the activity of an AGC protein kinase member other than PKA.

Cyclic nucleotide-free NO-dependent S-nitrosylation of specific proteins was confirmed on possible extracellular elements by both Western blot and immunohistochemistry in the *Helix pomatia* PC. Although the physiological relevance of S-nitrosylation has been shown in several proteins [79], there has been an active debate on its role in the nervous system among NO researchers [50]. One possible function of S-nitrosylation may be neuroprotection via the elimination of excess NO which would otherwise promote oxidative stress [80]. Alternatively, in tissues where NO signaling lacks a cGMP component, as shown in the internal neuropil of the *Limax* PC, S-nitrosylation is also suggested to be involved in the effector function of NO [42]. Basal protein S-nitrosylation, and NMDA stimulated S-nitrosylation of tubulin in the optic lobe of *Sepia*, also suggest the presence of NO-elicited protein modification in mollusks [63].

4.4. AGC-kinase dependent protein phosphorylation after odor exposition

In vivo experiments revealed potential NO/cGMP target protein phosphorylation events in the PC when animals were exposed to different odor stimuli. A marked increase in the phosphorylation level of the 28 kDa mw protein, which was also stimulated by cyclic nucleotide agonists ex vivo, was found when the animals encountered an attractive odor stimulus, suggesting that this protein might contribute to NO/cGMP induced molecular cascades underlying odor-elicited behavior. The number of snails exhibiting enhanced phosphorylation of this protein was maximal after the first encounter with the odor stimulus, and decreased once animals had started feeding, or if they re-encountered the appetitive odor three days after the first trial, or if they were exposed to a repellent odor stimulus. Similarly to our findings, NO was only involved in appetitive but not aversive olfactory learning [81]. In our behavioral experiments, the phosphorylation level of the 28 kDa protein changed parallel with the PC cGMP level, indicating that phosphorylation of the protein might follow the rise of cGMP level during odor perception. Considering the time window of cGMP accumulation and phosphorylation of the 28 kDa protein, it is assumed that the NO/cGMP induced phosphorylation regulates early events in odor information processing, and that these events are more characteristic of an initial encounter with the odor stimulus. Levels of hunger/motivation may also explain these observations, since animals who had already been introduced to the odor and consumed the food offered a few days earlier exhibited blunted phosphorylation events. This idea seems to be supported by the earlier observation that in näive, un-conditioned, *Helix pomatia* individuals, the food-finding ability of the animals was impaired when NOS was inhibited pharmacologically [67]. The 28 kDa protein is likely different to the small memory-related protein which is expressed in the *Limax* PC after taste aversion conditioning [82], because the two molecules differ in their mw and temporal activation. Interestingly, in the animals in which the 28 kDa protein showed enhanced phosphorylation, the phosphorylation level of higher molecular weight proteins, which were not affected by cyclic nucleotide agonists, was also elevated. These proteins might be involved in cyclic nucleotide-independent molecular events of olfactory information processing in the PC.

5. Conclusions

Summarizing our results, it can be concluded that the molecular events underlying odor processing and LFP oscillations are based on a NO-driven signaling in the *Helix pomatia* PC (Fig. 6). Accordingly, a subset of NB cells exhibiting moderate NOS activity can be stimulated by exogenous application of Glu and NMDA in low micromolar concentration. NO donors ex vivo, or an attractive in vivo odor stimulus, enhances cGMP synthesis, and induces the phosphorylation of a 28 kDa mw protein through an AGC protein kinase (possibly PKA). Therefore, a Glu (NMDA-receptor)–NO–cGMP–PKA–28 kDa mw protein phosphorylation pathway is suggested to be an important signal cascade during odor information processing in the *Helix pomatia* PC. Other shortcuts, such as direct S-nitrosylation of extracellular proteins by NO, activation of CNG channels in PC cells, and transcel-

lular activation of PKG containing neurons regulating tentacle positioning, are also suggested in the PC. To assess if these events occur concomitant with, or independently from, the NO-cGMP-PKA signaling pathway in the PC, needs further investigations.

Uncited reference

[36]

Acknowledgements

Authors are indebted to Katalin Ihász for her excellent technical help in behavioral experiments and Western blotting, and to Zsuzsanna N. Fekete for her skilled assistance in tissue preparation and immunohistochemical experiments. Dr. Daniel Fulton (University of Birmingham) is greatly acknowledged for expert, English language and grammar assistance. This study was supported by OTKA grants, Nos. PD75276 (Z.S.), and K78224, K111990 (K.E.), and a János Bolyai Research Scholarship, BO/00701/11, of the Hungarian Academy of Sciences (Z.S.).

References

[1] R. Chase, Food finding, In: Behavior and its Neural Control in Gastropod Molluscs, Oxford University Press, New York, 2002, pp. 130–141.
[2] S.F. Cummins, R.S. Wyeth, Olfaction in gastropods, in: A. Di Cosmo, W. Winlow (Eds.), Neuroecology and Neuroethology in Molluscs, Nova Science Publishers Inc., Hauppauge, 2014, pp. 45–71.
[3] S. Watanabe, Y. Kirino, A. Gelperin, Neural and molecular mechanisms of microcognition in Limax, Learn. Mem. 15 (2008) 633–642.
[4] E.I. Samarova, P.M. Balaban, Recording of spontaneous oscillations in the procerebrum of the terrestrial snail Helix during free behavior, Neurosci. Behav. Physiol. 37 (2007) 773–777.
[5] R. Chase, B. Tolloczko, Tracing neural pathways in snail olfaction: from the tip of the tentacles to the brain and beyond, Microsc. Res. Tech. 24 (1993) 214–230.
[6] R. Chase, R. Kamil, Neuronal elements in snail tentacles as revealed by horseradish peroxidase backfilling, J. Neurobiol. 14 (1983) 29–42.
[7] O.V. Zaitseva, Structural organization of the sensory systems of the snail, Neurosci. Behav. Physiol. 24 (1994) 47–57.
[8] S. Ratté, R. Chase, Morphology of interneurons in the procerebrum of the snail Helix aspersa, J. Comp. Neurol. 384 (1997) 359–372.
[9] V.N. Ierusalimsky, P.M. Balaban, Two morphological sub-systems within the olfactory organs of a terrestrial snail, Brain Res. 1326 (2010) 68–74.
[10] L. Hernádi, T. Teyke, Neuronal background of positioning of the posterior tentacles in the snail Helix pomatia, Cell Tissue Res. 352 (2013) 217–225.
[11] K.R. Delaney, A. Gelperin, M.S. Fee, J.A. Flores, R. Gervais, D.W. Tank, D. Kleinfeld, Waves and stimulus-modulated dynamics in an oscillating olfactory network, Proc. Natl. Acad. Sci. 91 (1994) 669–673.
[12] D. Kleinfeld, K.R. Delaney, M.S. Fee, J.A. Flores, D.W. Tank, A. Gelperin, Dynamics of propagating waves in the olfactory network of a terrestrial mollusc: an electrical and optical study, J. Neurophysiol. 72 (1994) 1402–1419.
[13] A. Gelperin, D.W. Tank, Odor-modulated collective network oscillations of olfactory interneurons in a terrestrial mollusc, Nature 345 (1990) 437–440.
[14] T. Inoue, S. Watanabe, S. Kawahara, Y. Kirino, Phase-dependent filtering of sensory information in the oscillatory olfactory center of a terrestrial mollusk, J. Neurophysiol. 84 (2000) 1112–1115.
[15] S. Watanabe, S. Kawahara, Y. Kirino, Morphological characterization of the bursting and nonbursting neurons in the olfactory centre of the terrestrial slug Limax marginatus, J. Exp. Biol. 201 (1998) 925–930.
[16] M. Murakami, S. Watanabe, T. Inoue, Y. Kirino, Odor-evoked responses in the olfactory center neurons in the terrestrial slug, J. Neurobiol. 58 (2004) 369–378.
[17] A. Gelperin, J. Flores, Vital staining from dye-coated microprobes identifies new olfactory interneurons for optical and electrical recording, J. Neurosci. Methods 72 (1997) 97–108.
[18] C.L. Sahley, K.A. Martin, A. Gelperin, Odors can induce feeding motor responses in the terrestrial mollusc Limax maximus, Behav. Neurosci. 106 (1992) 563–568.
[19] B. Ermentrout, J.W. Wang, J. Flores, A. Gelperin, Model for transition from waves to synchrony in the olfactory lobe of Limax, J. Comput. Neurosci. 17 (2004) 365–383.
[20] S. Ratté, R. Chase, Synapse distribution of olfactory interneurons in the procerebrum of the snail Helix aspersa, J. Comp. Neurol. 417 (2000) 366–384.
[21] O.V. Zaitseva, I.P. Ivanova, E.L. Luk'yanova, Ultrastructure of the area of procerebrum cell bodies in snails and slugs, J. Evol. Biochem. Physiol. 36 (2000) 421–431.
[22] K. Elekes, I. Battonyai, S. Kobayashi, E. Ito, Organization of the procerebrum in terrestrial pulmonates (Helix, Limax) reconsidered: cell mass layer synaptology and its serotonergic input system, Brain Struct. Funct. 218 (2013) 477–490.
[23] R. Matsuo, S. Kobayashi, S. Watanabe, S. Namiki, S. Iinuma, H. Sakamoto, K. Hirose, E. Ito, Glutamatergic neurotransmission in the procerebrum (olfactory center) of a terrestrial mollusk, J. Neurosci. Res. 87 (2009) 3011–3023.
[24] I.R.C. Cooke, A. Gelperin, Distribution of GABA-like immunoreactive neurons in the slug Limax maximus, Cell Tissue Res. 253 (1988) 77–81.
[25] L. Hernádi, Distribution and anatomy of GABA-like immunoreactive neurons in the central and peripheral nervous system of the snail Helix pomatia, Cell Tissue Res. 277 (1994) 189–198.
[26] A. Gelperin, Nitric oxide mediates network oscillations of olfactory interneurons in a terrestrial mollusk, Nature 369 (1994) 61–63.
[27] K. Nacsa, K. Elekes, Z. Serfőző, Immunodetection and localization of nitric oxide synthase in the olfactory center of the terrestrial snail, Helix pomatia, Acta Biol. Hung. 63 (Suppl. 2) (2012) 104–112.
[28] K. Nacsa, K. Elekes, Z. Serfőző, Ultrastructural localization of NADPH diaphorase and nitric oxide synthase in the neuropils of the snail CNS, Micron 75 (2015) 58–66.
[29] R. Matsuo, S. Kobayashi, K. Wakiya, M. Yamagishi, M. Fukuoka, E. Ito, The cholinergic system in the olfactory center of the terrestrial slug Limax, J. Comp. Neurol. 522 (2014) 2951–2966.
[30] R. Matsuo, R. Fukata, M. Kumagai, A. Kobayashi, S. Kobayashi, Y. Matsuo, Distribution of histaminergic neurons and their modulatory effects on oscillatory activity in the olfactory center of the terrestrial slug Limax, J. Comp. Neurol. 524 (2016) 119–135.
[31] I.R.C. Cooke, A. Gelperin, Distribution of FMRFamide-like immunoreactivity in the nervous system of the slug Limax maximus, Cell Tissue Res. 253 (1988) 69–76.
[32] K. Elekes, D.R. Nässel, Distribution of FMRFamide-like immunoreactive neurons in the central nervous system of the snail Helix pomatia, Cell Tissue Res. 262 (1990) 177–190.
[33] L. Hernádi, Y. Terano, Y. Muneoka, T. Kiss, Distribution of catch-relaxing peptide (CARP)-like immunoreactive neurons in the central and peripheral nervous system of Helix pomatia, Cell Tissue Res. 280 (1995) 335–348.
[34] K. Elekes, Ultrastructural aspects of peptidergic modulation in the peripheral nervous system of Helix pomatia, Microsc. Res. Tech. 49 (2000) 534–546.
[35] K. Elekes, T. Kiss, Y. Fujisawa, L. Hernádi, L. Erdélyi, Y. Muneoka, Mytilus inhibitory peptides (MIP) in the central and peripheral nervous system of the pulmonate gastropods Lymnaea stagnalis and Helix pomatia: distribution and physiological actions, Cell Tissue Res. 302 (2000) 115–134.
[36] A. Gelperin, Oscillatory dynamics and information processing in olfactory systems, J. Exp. Biol. 202 (1999) 1855–1864.
[37] T. Inoue, S. Watanabe, Y. Kirino, Serotonin and NO complementarily regulate generation of oscillatory activity in the olfactory CNS of a terrestrial mollusk, J. Neurophysiol. 85 (2001) 2634–2638.
[38] T. Inoue, Y. Inokuma, S. Watanabe, Y. Kirino, In vitro study of odor-evoked behavior in a terrestrial mollusk, J. Neurophysiol. 9 (2004) 372–381.
[39] S. Kobayashi, M. Hattori, E. Ito, The effects of GABA on the network oscillations of the procerebrum in Limax valentianus, Acta Biol. Hung. 59 (2008) 77–79.
[40] S. Kobayashi, M. Hattori, K. Elekes, E. Ito, R. Matsuo, FMRFamide regulates oscillatory activity of the olfactory center of the slug, Eur. J. Neurosci. 32 (2010) 1180–1192.
[41] S. Fujie, H. Aonuma, I. Ito, A. Gelperin, E. Ito, The nitric oxide/cyclic GMP pathway in the olfactory processing system of the terrestrial slug Limax marginatus, Zool. Sci. 19 (2002) 15–26.
[42] S. Fujie, T. Yamamoto, J. Murakami, D. Hatakeyama, H. Shiga, N. Suzuki, E. Ito, Nitric oxide synthase and soluble guanylyl cyclase underlying the modulation of electrical oscillations in a central olfactory organ, J. Neurobiol. 62 (2005) 14–30.
[43] R. Matsuo, E. Ito, A novel nitric oxide synthase expressed specifically in the olfactory center, Biochem. Biophys. Res. Commun. 386 (2009) 724–728.
[44] S. Watanabe, S. Kawahara, Y. Kirino, Glutamate induces Cl^- and K^+ currents in the olfactory interneurons of a terrestrial slug, J. Comp. Physiol. A. 184 (1999) 553–562.
[45] S. Watanabe, Y. Kirino, Selective calcium imaging of olfactory interneurons in a land mollusk, Neurosci. Lett. 417 (2007) 246–249.
[46] T.J. Ha, A.B. Kohn, Y.V. Bobkova, L.L. Moroz, Molecular characterization of NMDA- like receptors in Aplysia and Lymnaea: relevance to memory mechanisms, Biol. Bull. 210 (2006) 255–270.
[47] L.L. Moroz, J. Győri, J. Salánki, NMDA-like receptors in the CNS of molluscs, Neuroreport 4 (1993) 201–204.

[48] T.L. Dyakonova, V.E. Dyakonova, Modification of the effects of glutamate by nitric oxide (NO) in a pattern-generating network, Neurosci. Behav. Physiol. 38 (2008) 407–413.
[49] T.L. Dyakonova, V.E. Dyakonova, Participation of receptors of the NMDA type in regulation by glutamate of alimentary motor program of the freshwater mollusc Lymnaea stagnalis, J. Evol. Biochem. Physiol. 46 (2010) 53–60.
[50] J. Garthwaite, Concepts of neural nitric oxide-mediated transmission, Eur. J. Neurosci. 27 (2008) 2783–2802.
[51] S.H. Francis, J.L. Busch, J.D. Corbin, cGMP-dependent protein kinases and cGMP phosphodiesterases in nitric oxide and cGMP action, Pharmacol. Rev. 62 (2010) 525–563.
[52] S.A. Bradley, J.R. Steinert, Nitric oxide-mediated posttranslational modifications: impacts at the synapse, Oxidative Med. Cell. Longev. (2016)5681036http://dx.doi.org/10.1155/2016/5681036.
[53] N. Andreakis, S. D'Aniello, R. Albalat, F.P. Patti, J. Garcia-Fernàndez, G. Procaccini, P. Sordino, A. Palumbo, Evolution of the nitric oxide synthase family in metazoans, Mol. Biol. Evol. 28 (2011) 163–179.
[54] L.L. Moroz, A.B. Kohn, Parallel evolution of nitric oxide signaling: diversity of synthesis and memory pathways, Front. Biosci. 16 (2011) 2008–2051.
[55] K. Welshhans, V. Rehder, Nitric oxide regulates growth cone filopodial dynamics via ryanodine receptor-mediated calcium release, Eur. J. Neurosci. 26 (2007) 1537–1547.
[56] M. Ribeiro, V.A. Straub, M. Schofield, J. Picot, P.R. Benjamin, M. O'Shea, S.A. Korneev, Characterization of NO-sensitive guanylyl cyclase: expression in an identified interneuron involved in NO–cGMP-dependent memory formation, Eur. J. Neurosci. 28 (6) (2008) 1157–1165.
[57] M. Ribeiro, M. Schofield, I. Kemenes, P.R. Benjamin, M. O'Shea, S.A. Korneev, Atypical guanylyl cyclase from the pond snail, Lymnaea stagnalis: cloning, sequence, analysis and characterization of expression, Neuroscience 165 (2010) 794–800.
[58] I. Kemenes, G. Kemenes, R.J. Andrew, P.R. Benjamin, M. O'Shea, Critical time-window for NO-cGMP-dependent long-term memory formation after one-trial appetitive conditioning, J. Neurosci. 22 (4) (2002) 1414–1425.
[59] G. Kemenes, Molecular mechanisms of associative learning in Lymnaea, in: J.H. Byrne (Ed.), Learning and Memory - A Comprehensive Reference, Elsevier, Oxford, 2008, pp. 133–148.
[60] U. Müller, The molecular signalling processes underlying olfactory learning and memory formation in honeybees, Apidologie 43 (3) (2012) 322–333.
[61] B.D. Manning, L.C. Cantley, AKT/PKB signaling: navigating downstream, Cell 129 (2007) 1261–1274.
[62] Q. Yang, P. Kuzyk, I. Antonov, C.J. Bostwick, A.B. Kohn, L.L. Moroz, R.D. Hawkins, Hyperpolarization-activated, cyclic nucleotide-gated cation channels in Aplysia: contribution to classical conditioning, Proc. Natl. Acad. Sci. U. S. A. 112 (2015) 16030–16035.
[63] A. Palumbo, G. Fiore, C. Di Cristo, A. Di Cosmo, M. d'Ischia, NMDA receptor stimulation induces temporary alpha-tubulin degradation signaled by nitric oxide-mediated tyrosine nitration in the nervous system of Sepia officinalis, Biochem. Biophys. Res. Commun. 293 (2002) 1536–1543.
[64] I.R. Cooke, S.L. Edwards, C.R. Anderson, The distribution of NADPH diaphorase activity and immunoreactivity to nitric oxide synthase in the nervous system of the pulmonate mollusc Helix aspersa, Cell Tissue Res. 277 (1994) 565–572.
[65] S. Huang, H.H. Kerschbaum, E. Engel, A. Hermann, Biochemical characterization and histochemical localization of nitric oxide synthase in the nervous system of the snail, Helix pomatia, J. Neurochem. 69 (1997) 2516–2528.
[66] S. Huang, H.H. Kerschbaum, A. Hermann, Nitric oxide-mediated cGMP synthesis in Helix neural ganglia, Brain Res. 780 (1998) 329–336.
[67] T. Teyke, Nitric oxide, but not serotonin, is involved in acquisition of food-attraction conditioning in the snail Helix pomatia, Neurosci. Lett. 206 (1996) 29–32.
[68] T. Mattiello, G. Fiore, E.R. Brown, M. d'Ischia, A. Palumbo, Nitric oxide mediates the glutamate-dependent pathway for neurotransmission in Sepia officinalis chromatophore organs, J. Biol. Chem. 285 (2010) 24154–24163.
[69] M. Peschel, V. Straub, T. Teyke, Consequences of food-attraction conditioning in Helix: a behavioral and electrophysiological study, J. Comp. Physiol. A. 178 (1996) 317–327.
[70] M. Lemaire, R. Chase, Twitching and quivering of the tentacles during snail olfactory orientation, J. Comp. Physiol. A. 182 (1998) 81–87.
[71] J. Tanaka, M. Markerink-van Ittersum, H.W. Steinbusch, J. De Vente, Nitric oxide-mediated cGMP synthesis in oligodendrocytes in the developing rat brain, Glia 19 (1997) 286–297.
[72] S. Watanabe, F. Takanashi, K. Ishida, S. Kobayashi, Y. Kitamura, Y. Hamasaki, M. Saito, Nitric oxide-mediated modulation of central network dynamics during olfactory perception, PLoS One 10 (9) (2015)e0136846http://dx.doi.org/10.1371/journal.pone.0136846.
[73] R. Matsuo, K. Misawa, E. Ito, Genomic structure of nitric oxide synthase in the terrestrial slug is highly conserved, Gene 415 (2008) 74–81, http://dx.doi.org/10.1016/j.gene.2008.02.021.
[74] Z. Pirger, I. Battonyai, N. Krajcs, K. Elekes, T. Kiss, Voltage-gated membrane currents in neurons involved in odor information processing in snail procerebrum, Brain Struct. Funct. 219 (2014) 673–682.
[75] S.R. Vincent, J.A. Williams, P.B. Reiner, A.E. El-Husseini, Monitoring neuronal NO release in vivo in cerebellum, thalamus and hippocampus, Prog. Brain Res. 118 (1998) 27–35.
[76] I. Battonyai, N. Krajcs, Z. Serfőző, T. Kiss, K. Elekes, Potassium channels in the central nervous system of the snail, Helix pomatia: localization and functional characterization, Neuroscience 268 (2014) 87–101, http://dx.doi.org/10.1016/j.neuroscience.2014.03.006.
[77] J.H. Park, V.A. Straub, M. O'Shea, Anterograde signalling by nitric oxide: characterization and in vitro reconstitution of an identified nitrergic synapse, J. Neurosci. 18 (1998) 5463–5476.
[78] J.W. Jacklet, D.G. Tieman, Nitric oxide and histamine induce neuronal excitability by blocking background currents in neuron MCC of Aplysia, J. Neurophysiol. 91 (2004) 656–665.
[79] N. Gould, P.T. Doulias, M. Tenopoulou, K. Raju, H. Ischiropoulos, Regulation of protein function and signaling by reversible cysteine S-nitrosylation, J. Biol. Chem. 13 (288) (2013) 26473–26479.
[80] T. Nakamura, S.A. Lipton, Protein S-nitrosylation as a therapeutic target for neurodegenerative diseases, Trends Pharmacol. Sci. 37 (2016) 73–84.
[81] T. Yabumoto, F. Takanashi, Y. Kirino, S. Watanabe, Nitric oxide is involved in appetitive but not aversive olfactory learning in the land mollusk Limax valentianus, Learn. Mem. 15 (2008) 229–232.
[82] T. Nakaya, S. Kawahara, S. Watanabe, D. Lee, T. Suzuki, Y. Kirino, Identification and expression of a novel gene in odour-taste associative learning in the terrestrial slug, Genes Cells 6 (2001) 43–56.